8-2024

Interaction Of Cellulose Model (D-Cellobiose) With Some Selected Sodium Salts

Uchechukwu G. Ariwodo

INTERACTION OF CELLULOSE MODEL (D-CELLOBIOSE) WITH SOME SELECTED SODIUM SALTS

A Thesis

By

UCHECHUKWU G ARIWODO

Submitted to the Office of Graduate Studies of
Prairie View A&M University
in partial fulfillment of the requirements for the degree of

MASTER OF SCIENCE

August 2024

Major Subject: Chemistry

INTERACTION OF CELLULOSE MODEL (D-CELLOBIOSE) WITH SOME SELECTED SODIUM SALTS

A Thesis

By

UCHECHUKWU G ARIWODO

Submitted to the Office of Graduate Studies of
Prairie View A&M University
in partial fulfillment of the requirements for the degree of

Approved as to style and content by:

Ananda Amarasekara Chair of Committee	Harshica Fernando Co-Chair of Committee
Sameh Abdelwahed Committee Member	Ananda Amarasekara Head of Department
Mathew Minus Committee Member	Dorie J. Gilbert Dean of the College of Arts & Sciences

Tyrone Tanner
Dean of Graduate Studies

August 2024

Major Subject: Chemistry

ABSTRACT

Modification and Interaction of Cellulose Model (d-cellobiose) with some Selected Sodium Salts

(August 2024)

Uchechukwu G Ariwodo, B.S., Abia State University; M.S., Prairie View A&M University.

Chair of Advisory Committee: Dr. Ananda Amarasekara

This work focused on employing sodium salts to modify cellulose, a crucial biopolymer found in plant cell walls, to improve its characteristics. Three methods were used to study cellulose-salt interaction. Task 1 employed Fourier-transform infrared spectroscopy (FT-IR) to examine infrared absorption frequencies and discovered that the highest peak shift was caused by sodium borate (Na_3BO_3). In Task 2, thermal stability was evaluated using thermogravimetric analysis. The results showed that while sodium sulfate (Na_2SO_4) decreased stability and combustion temperature, sodium bicarbonate ($NaHCO_3$) increased both. Task 3 investigated interactions between cellobiose and sodium salts using density functional theory and computational techniques, with a particular emphasis on bond lengths ≤ 3.5 Å. Sodium borate (Na_3BO_3) had strong binding at 1.780 Å, whereas sodium azide (NaN_3) had the maximum binding activity with a bond length of 1.882 Å. According to estimations of reaction energy, sodium borate, and β-cellobiose had the maximum energy at 30.88 Kcal/mol, while sodium nitrite and α-cellobiose had the lowest energy at -97 Kcal/mol. This study shows the influence of sodium salt on cellulose.

***Keywords*:** cellulose, biopolymer, Cellobiose, sodium salts, bond length

DEDICATION

The result of numerous, difficult sacrifices is in this work. This work, through my efforts, is sincerely and proudly dedicated to the individuals who inspired me, from parents and guardians to classmates and my circle of friends who helped when I ran into difficulties while working on this project. Additionally, to Prairie View A&M University's faculty and staff. Above all, we are grateful to our All-Powerful God, who bestows blessings upon us every day, especially for the courage, strength, wisdom, time, patience, and direction we have needed to complete this task.

ACKNOWLEDGMENTS

For his guidance and research training, I am extremely appreciative of my supervising professor, Dr. Ananda Amarasekara. Considering the excellent influence, he has had on my life during my time at Prairie View A&M University, it was a true honor to meet and collaborate with him. Thank you also to Drs. Sameh Abdelwahed, Harschica Fernando, and Mathew Minus for their technical assistance, mentorship, and support throughout my research project. Additionally, I would like to extend my gratitude to the faculty and staff of the Chemistry department. To Drs. Gina, Andrea, Neelgund, Gao, Mr. Tony, Marco Giles, Li, Ms. Wilson, Liu, Aida, Esther, Mohamed, Rashid, and Tefera, for their warm gestures and selfless advice during my master's program in Chemistry.

I would especially like to thank Dr. Doris Gilbert, Dean of Brailsford College of Arts & Sciences, for all her support, kindness, and guidance during my program. Thanks again to the National Science Foundation (NSF) for providing money for the research for this thesis. I also sincerely thank all my wonderful friends, especially Dr. Caleb, Victor, Jennifer Nnaemeka, Bright, Chujor, and all my colleagues who stood by me throughout my master's program. In addition, I would like to use this opportunity to thank Ms. Victoria, Mrs. Asia, STEM Program Coordinator, and everyone, who in one way or another has made my time at Prairie View A&M University worthwhile.

TABLE OF CONTENT

Page

LIST OF FIGURES

FIGURE Page

LIST OF TABLES

TABLE Page

NOMENCLATURE

LIST OF SYMBOLS, ABBREVIATIONS, OR ACRONYMS

DP	Degree of polymerization
AGU	Anhydroglucopyroniose
IL	Ionic liquids
CA	Cellulose acetate
CS	Cellulose sulfate
DS	Degree of substitution
CMC	Carboxymethylcellulose
MC	Methylcellulose
EC	Ethylcellulose
HEC	Hydroxy ethyl cellulose
HPC	Hydroxypropyl cellulose
HEMC	Hydroxy ethyl methylcellulose
NMMO	N-methyl morpholine-N-oxide
BMIMCL	1-butyl-3-methylimidazolium chloride
EMIMCL	1-ethyl-3-methylimidazolium chloride
IE	Individual energy
CE	Cellobiose energy

CHAPTER 1

INTRODUTION

Polysaccharides are the most prevalent natural biopolymers with unique chemical, physical, and biological characteristics. The backbone of these polymers is made up of monosaccharide building units and glycosidic connections, which also define the variety and complexity of the polysaccharide(Gu & Doner, 1992). Since polysaccharides were initially used in medicine and discovered to have bioactivities (Goebel & Adams, 1943), numerous academics have focused their research on polysaccharides derived from various sources. Numerous studies have demonstrated the wide range of qualities that various polysaccharides derived from microbes, plants, and animals possess, including antioxidant, immune-regulating, anti-inflammatory, anti-HIV, antimutagenic, anticancer, and anticoagulant actions (Ukai et al., 1983).

Although the bioactivities of natural polysaccharides are desirable, they are only sometimes satisfactory. Researchers have discovered the following regarding polysaccharide structure-activity relationships: first, not all naturally occurring polysaccharides have bioactivities; untreated pachymaran, for example, has no bioactivity (Gao et al., 2005). Second, some polysaccharides are unsuitable for exerting bioactivities due to their structure and physicochemical characteristics.

This thesis (dissertation) follows the style of the *American Psychological Association, 7th Ed*

The molecular weight of bioactive polysaccharides is too high, making it difficult for them to cross various cell membrane barriers and impact organisms (Alban & Franz, 2000). Conversely, polysaccharides will not exhibit bioactivities if the molecular weight is too low. The structural alteration of substances by chemical, physical, and biological processes to produce various derivative structures is known as molecular modification. Structure alterations can be used to change physicochemical characteristics and biological activities. In addition to enriching the varieties of polysaccharide compounds and giving researchers additional alternatives for screening biological activity or specific polysaccharide agents, will enable better analysis of the structure-activity connections.

Some researchers have obtained desirable modified polysaccharides, most of which have the appropriate characteristics to work with pharmacological effects more effectively. Research has demonstrated that the bioactivities of natural polysaccharides are connected to their inherent characteristics, such as the kinds of glycosidic bonds and solubility (Lu et al., 2012), relative molecular mass (Li & Wang, 1994), main-chain configuration (Hattori et al., 1998), and spatial configuration (Wang et al., 2013). The most crucial of them are the different kinds of glycosidic bonds, the connections between them, and the compositions of the monosaccharides because these are the factors that define whether a polysaccharide has bioactivities.

In contrast, others can merely impact the levels of bioactivities. The former is the inherent qualities of polysaccharides that cannot be altered; however, the rest can be altered using the proper modification techniques. Therefore, investigations focusing on modifying polysaccharides and synthesizing polysaccharides with optimum bioactivities have been conducted based on the structure-activity relationship (Siddiqui & Cavicchioli, 2005). The types, numbers, and positions of the substituent groups in polysaccharides might all be altered

through molecular modification, affecting the bioactivities. Numerous molecular modification techniques have been developed so far such as carboxymethylation, (Chen et al., 2014), sulfation (Wang et al., 2013), selenization (Qiu et al., 2014), phosphorylation (Ye et al., 2013), and ultrasonic disruption (Zhang et al., 2013), and polysaccharide degradation are categorized as chemical, physical, and biological alterations.

By adding substituent groups to polysaccharide structures, chemical modification is a popular technique that can enhance the original polysaccharides' bioactivities and provide new, valuable bioactivities. Sulfation, alkylation, carboxymethylation, phosphorylation, selenization, and acetylation are examples of chemical modification techniques.

To produce fragments with lower molecular weights, the physical modification approach truncates the original polysaccharide backbone. By using this technique, the fundamental structure of polysaccharides could be preserved with only minor conformational alterations. The most popular techniques include microwave exposure, radiation-induced response, and ultrasonic disruption. In general, "biological modification of polysaccharides" refers to the catalytic destruction of polysaccharides using enzymes. Enzymatic modification has the benefits of high specificity, high efficiency, and few adverse effects compared to chemical modification. After enzymatic degradation, the relative molecular weights of polysaccharide derivatives are generally consistent, which would not significantly affect the main chain of a polysaccharide. Enzymatic degradation mainly involves breaking down the polysaccharide's backbone before lowering its molecular weight and viscosity (Oosterveld et al., 2002).

Several methodologies have been used over the last 20 years to identify polysaccharides' three-dimensional "relaxed" structure. Although computer power and calculation speeds have increased exponentially, the most sophisticated techniques, such as quantum mechanical

methods (ab initio methods), do not help deal with the complexity of many-particle systems like they are for macromolecular media. These techniques, on the other hand, have been successfully applied to small molecules, such as mono and disaccharides, for predicting charge distribution, preferred conformations, and transitions among accessible conformations, providing background knowledge for more complicated systems (Burton & Brant, 1983).

Rotation about glycosidic links produces prominent features in the molecular topology and flexibility of disaccharides and higher oligosaccharides (Burton & Brant, 1983). The conformational analysis aims to calculate the probability, that is energy, of all mutual orientations of two neighboring monosaccharide units as a function of rotations about glycosidic links specified by dihedral angles ϕ and Ψ. As a result, it was formerly customary to compute the conformational energy solely as a function of dihedral angles ϕ and ψ, assuming the sugar ring to be rigid (rigid residual model). The rigid-residue approach is still considered a valid starting point in the conformational study of polysaccharides if the coordinates of all atoms in the monomeric unit have been computed using an appropriate independent method (Ruggiero et al., 1995).

As the world's most prevalent bio-renewable and biodegradable organic polymeric compound, cellulose is recognized as a virtually limitless source of raw materials to produce environmentally friendly and biocompatible goods (Nishiyama et al., 2002; Ragauskas et al., 2006; Solomon et al., 2007;). It is extensively used in many industries, including the paper, pulp, film, filter, and textile sectors (Isobe et al., 2013). However, its applications are restricted because cellulose cannot be melted or dissolved in typical solvents. The highly developed cellulose's intra- and intermolecular hydrogen bonding networks primarily cause insolubility (Heinze, 1998; Heinze & Liebert, 2001; Klemm et al., 2005).

Cellulose modification and the creation of regenerated cellulose products depend heavily on cellulose dissolution. Aqueous and non-aqueous solvents, as well as derivative and non-derivative solvents, are two categories for cellulose solvents. It is common knowledge that salts have an impact on non-derivative salt aqueous solutions used to dissolve cellulose. Only an aqueous solution containing 55% (w/w) of $ZnCl_2$ may cause cellulose to swell, but an aqueous solution containing 63% (w/w) of $ZnCl_2$ can dissolve cellulose (Letters, 1932). Other efficient solvents for cellulose include Ca(SCN)2/H_2O (Hattori et al., 1998), LiSCN/H_2O (Fischer et al., 2003), and LiBr/H2O (Yang et al., 2002).

Inorganic molten salt hydrates and their combinations have garnered significant interest recently as potential novel solvents or media for polysaccharide modification. It takes 40 minutes at 120–140 °C for cellulose to dissolve in Ca(SCN)2·3H2O (Kuga, 1980). Ca2+, which can attack cellulose's oxygen atoms at O_5 and O_6 to form a five-membered ring and break cellulose hydrogen bonds, is the cause of the breakdown, according to IR, 13C-, and ^{1}H-NMR tests. Concurrently, two SCN− groups and two water molecules join forces with Ca2+ to accomplish its 6-valence coordination (Hattori et al., 1998).

Using 2D 7Li–1H heteronuclear Overhauser effect spectroscopy (HOESY), direct interactions between the Li+ and hydroxyl groups of cellulose are seen; cations and anions from the salt engage with hydroxyl groups of cellulose to break hydrogen bonds (Fischer et al., 2003). The main topic of discussion regarding the cellulose dissolution mechanism in molten salt systems has been whether the hydroxyl groups of the cellulose contribute to the cation coordination (Medronho & Lindman, 2014). The interactions of various pure molten salt hydrates and salt mixes with cellulose have been studied.

Because of the intricacy of the cellulose structure, transmittance, calorimetry, and ^{1}H NMR were utilized to investigate the interactions between cellulose and salt-aqueous solutions using the repeat unit D-cellobiose. The interactions and dissolving behaviors of cellobiose in aqueous solutions of water, $ZnCl_2$, LiCl, NaCl, KCl, and NH_4Cl were studied. It was discovered for the first time that the ionic effects on the dissolution of cellobiose in salt-aqueous solutions follow the Hofmeister series. This study established the precise ionic impacts on cellobiose's water solubility and offered essential data for comprehending cellulose's dissolution in salt-aqueous solutions.

1.1 **Aim and Objectives of the Research**

The research aimed to characterize the behavior of a modified form of cellobiose with some selected sodium salts. Such behavior includes:

i) Peak shifts between the cellobiose and salt samples.

ii) Thermal stability and rate of decomposition of the cellobiose-salt mixture regarding pure cellobiose.

iii) Binding position of the sodium ion(s) of the salt with the cellulose model.

iv) Energies of the reactions and free binding energies of the reaction.

2 LITERATURE REVIEW

2.1 **Overview of Cellulose**

In nature, cellulose is a readily available and renewable biopolymer frequently found with lignin and hemicelluloses in the cell walls of higher plant sections (Olsson & Westman, 2013). β(1-4) glycosidic linkages connect condensed d-glucose units linearly to produce this homopolysaccharide. The degree of polymerization (DP), which ranges from 100 to 2000033, may vary greatly depending on the source. The organization of cellulose is complicated, ranging from the single anhydroglucopyranose unit (AGU) to the micro and macro fibrils. The basis of cohesion between cellulose molecules (see Fig. 1) is considered a broad intra- and intermolecular network of hydrogen bonds.

While intermolecular hydrogen bonds enable the linear polymer molecules to form in configurations resembling sheets, intramolecular hydrogen bonds are thought to provide chains with their stiffness (Klemm et al., 2005). A more contemporary viewpoint emphasizes cellulose's amphiphilic properties (Lindman et al., 2010; Medronho et al., 2012; Medronho & Lindman, 2014). A glucopyranose ring's equatorial direction is hydrophilic due to all three hydroxyl groups in these places. However, because the hydrogen atoms in C–H bonds are positioned on the axial positions of the ring, the ring's axial direction is hydrophobic. As a result, the flat ribbons on cellulose molecules have an inherent structural anisotropy, with distinct polarity differences on either side (Biermann et al., 2001; Miyamoto et al., 2009; Yamane et al., 2006). Although this structural anisotropy has generally been disregarded in most debates, it is expected to impact cellulose's macroscopic and microscopic characteristics significantly.

Figure 2. 1

Molecular Structure of Cellulose showing the Extended Network of Intra and Inter-Hydrogen Bonding and Anhydrocellobiose Unit

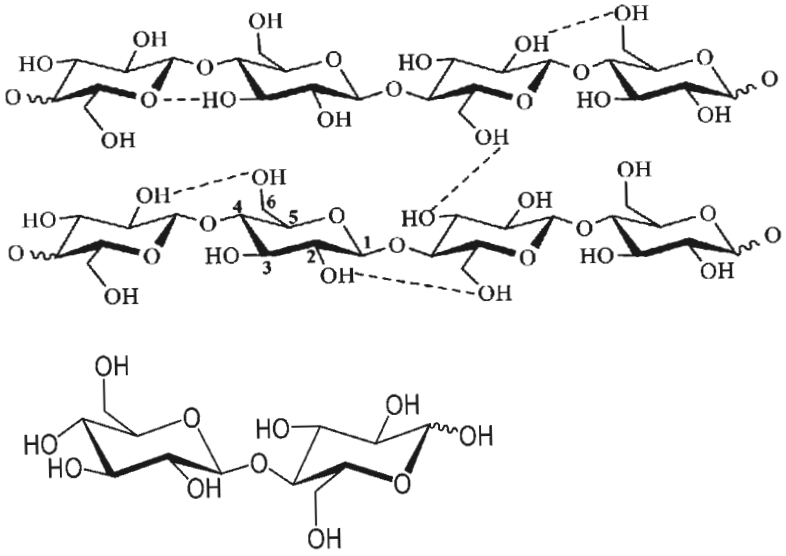

With lower-order amorphous regions coexisting with higher-order crystalline domains, cellulose can be considered a semi-crystalline polymer (Klemm et al., 1998). The degree of crystallinity in cellulose varies depending on its origin and pretreatments. It usually ranges from 40% to 60%. The so-called "fringed fibrillar model" is now widely accepted (Fink et al., 1995; Fink et al., 1994; Fink & Philipp, 1985; Hearle, 1958; Krässig, 1984; Lenz et al., 1993). Over the years, several theories have been established regarding how these crystalline and non-crystalline regions are intermixed. These theories have included single crystals and uniform elementary fibrils. The cellulose nanofibril is not considered a single crystal in this concept but rather a less ordered configuration with non-uniform crystalline segments paired with amorphous portions displaced laterally and longitudinally (Hearle, 1958).

2.2 Sources of cellulose

As seen in Figure 2, numerous sources of cellulose are found in nature, such as fungi, algae, bacteria, animals, trees, and annual plants. The primary source is plant fiber, where cellulose is a structural component that strengthens wood and other plants. Cellulose can occur in relatively pure forms, such as the cellulose content of cotton seed hairs, which exceeds 90% weight. However, most of the time, cellulose coexists with lignin, other polysaccharides like pectins and hemicelluloses (polyposis), and comparatively small amounts of organic compounds or extractives (Varshney & Naithani, 2011).

The sulfite and kraft (sulfate) processes are the most popular pulping processes, which separate cellulose from wood (Sixta et al., 2006). These processes result in pulps with different fiber strengths and purities, such as paper-grade pulp used for printing paper or dissolving grade pulp applied to produce regenerated cellulose and cellulose derivatives. Cellulose is partially liberated from lignin and another plant. components (like hemicelluloses) during these processes.

Figure 2. 2

Cellulose can be Obtained from Various Sources, some examples: (A) Beech tree, (B) Bamboo, (C) Cotton, (D) Sisal, (E) Tunicine, (F) Gluconacetobacter xylinum. Reproduced with permission from Ref. (Popa, 2011). Copyright (Figure 2F) Wiley

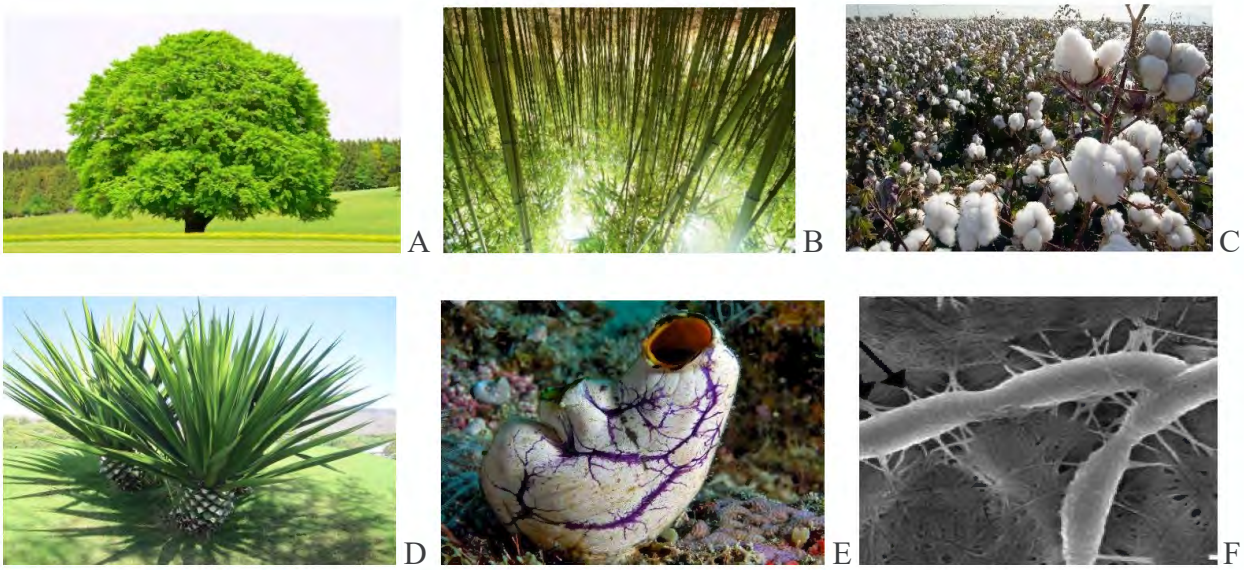

Plant cell walls are mainly made of cellulose, hemicelluloses, and lignin (Fig. 3). Lignin makes up approximately 10–25% of the dry weight of the cell walls and serves as a binder between the cellulose and hemicellulose components. Lignin protects the cell wall and provides stiffness and strength through its binding role. Regarding the dry weight of lignocellulosic biomass, cellulose, and hemicelluloses, two other essential components of plant cell walls account for roughly 35–50% and 20–35%, respectively.

Figure 2. 3

Structure of Plant Cell Wall in Lignocellulosic Biomass which consists of Lignin, Hemicellulose, and Cellulose

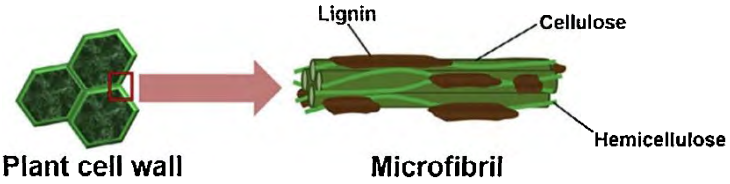

With repeating units of cellobiose (disaccharide D glucose) units linked by β-1,4 linkage, cellulose is a linear polysaccharide. Adjacent glucose units in the same or different chain exhibit strong intra- or intermolecular hydrogen bonding due to the open hydroxyl groups in glucose monomer units (Phanthong et al., 2018; Dufresne, 2012). Plant cell walls include hemicellulose, primarily in the form of xylans and glucomannans, and monomers of pentose and hexose connected by short or branching chains. The plant cell wall's toughness, strength, and water solvent impermeability are all attributed to the densely packed networks of hydrogen bonds in these compact hydrogen bonding structures.

Plant, animal, and mineral sources are the origins of natural fibers. Vegetable fiber, for instance, can be further divided into seed, stem, leaf, and other types. Petrochemicals and other synthetic materials are typically used to create synthetic textiles. Furthermore, several synthetic fibers, such as rayon, modal, and Lyocell, are also made from natural cellulose. Numerous methods, like cupro-ammonium, can regenerate cellulose into pure fibers. Cellulose can also be changed to become cellulose acetate fibers (Lavanya et al., 2011).

2.3 Applications of cellulose

In addition to being utilized in unaltered forms like cotton or wood, cellulose can be taken from its natural sources and utilized, on a lesser scale, in specific applications like regenerated fibers (like viscose or Lyocell) or the paper industry. Indeed, new ecological artificial fibers, such as cellulose derived from forests, can significantly replace cotton and fibers derived from fossil fuels in both woven and non-woven end applications. Creating novel solvents and dissolution and regeneration techniques is essential to the success of this replacement. Moreover, cellulose can be altered chemically, enzymatically, or microbiologically to produce new, valuable derivatives and materials. Numerous significant industrial sectors, including the paint, polymer, and membrane industries, use large-scale manufacture of cellulose derivatives, mostly ethers and esters, and regenerated materials, that is fibers, films, food packaging, membranes, and sponges, among others (Klemm et al., 2005).

The fact that cellulose must dissolve to be used in numerous significant applications presents a complex problem. Chemical processing of cellulose is quite challenging because of the extensive non-covalent connections among molecules, the partly crystalline structure, and the complexity of this biopolymeric network. Common aqueous and organic solvents do not dissolve or dissolve cellulose (Krässig, 1993; Marsh & Wood, 1945). This polysaccharide, however, has no prominent common characteristics and is soluble in more unusual media (Sixta et al. 2006). Leaders in the field have generally agreed that the solvent's ability to disrupt the intra- and intermolecular hydrogen bond network described above is the key to dissolving cellulose (Zhang et al., 2002).

Bionanocomposites made of cellulose have numerous uses in a range of sectors. The paper and packaging industries have embraced nanocellulose's prospective applications and biocomposites. Because of its high strength, stiffness, and nanoscale dimensions, cellulose-based nanocomposites have attracted much attention for use in a variety of industries, including construction, for the creation of structural composites, automotive, to produce parts based on micropatterns, electronics, as a membrane for electroacoustic devices, pharmacy, or biomedical applications, and cosmetics. Additionally, nanocellulose composites can be used as fuel cells, ion exchange, ultrafiltration, and other membrane applications. Over the past ten years, much research has been done on nanocellulose, which has many uses.

2.3.1 Composites and Fillers

When manufacturing nanocomposites, such as films, coatings, and foams, among other materials, nanocellulose offers intriguing qualities for usage as a reinforcing agent. Using potato starch as the polymer matrix and nanofiber cellulose as the reinforcing agent, Dufresne et al. initially reported on the enhanced mechanical capabilities of a nanocomposite. Nowadays, the use of nanocellulose as a reinforcing agent is well-established and backed by various literatures. Nakagaito and Yano (Nakagaito & Yano, 2008) observed improved tensile properties when phenol–formaldehyde resin was mixed with nanofiber cellulose, while (Zimmermann et al , 2017) reported comparable outcomes when hydroxypropylated cellulose (HPC) was used. Melamine formaldehyde (MF) was used to saturate nano paper, according to a recent publication by Henriksson et al. (Henriksson & Berglund, 2007).

Figure 2. 4

Potential Applications of Nanocellulose in Different Fields

2.3.2 Paper and Packaging Industry

The paper and packaging sectors use nanocellulose applications to replace synthetic polymers made from petrochemical resources (Lavoine et al., 2012). The unique properties of nanocellulose, including its size at the nanoscale and its ability to block gas and water, can be used to create nanocomposite films with strong construction networks that permit penetrant molecules to flow through (Nair et al., 2014). Additionally, because it comes from a naturally occurring, renewable source of cellulose, it is inexpensive and non-toxic, making it ideal for use in food packaging.

The development of a nano-biocomposites film with nano-clay and a polylactic acid (PLA) matrix containing nanocellulose as a reinforcing agent for use in food packaging has

been recently reported in the literature (Trifol et al., 2016). This led to a notable improvement in the film's water and oxygen barrier properties. For the development of such composite films with nanocellulose as the reinforcing polymer and better gas barrier and mechanical qualities for packaging, other options for the matrix include carboxymethyl guar (CMG), agar, or semi-interpenetrating polymer network of poly (vinyl alcohol)/polyacrylamide.

2.3.3 Biomedical Applications

Due to its unique qualities, such as its high strength, variable surface chemistry, and high surface area to volume ratio, nanocellulose is also used in the biomedical industry. The most effective use is in creating nanocellulose-reinforced hydrogel composites, which have the desired characteristics of both the host matrix and the reinforcement phases and can improve the mechanical properties in polymeric gel formulations (De France et al., 2017; Mandal & Chakrabarty, 2017). To create a novel hydrogel with enhanced pH sensitivity and mechanical capabilities for usage in novel pharmacological and gene delivery applications, Lavoine et al., 2012; Sampath et al., 2015) recently reported producing a novel hydrogel with a semi-interpenetrating polymer network. The development of an electrospun poly(ε-caprolactone)/nanocellulose composite fiber mat for use as a scaffold in tissue engineering applications was documented in a recent research publication (Si et al., 2016).

2.4 Cellulose solvents

The problem of cellulose's insoluble nature in water and typical organic solvents has been thoroughly studied; (Heinze & Koschella, 2005; Liebert, 2010; Schulz et al., 2000). Several reasons related to cellulose's chemical structure contribute to its insolubility. First, thermodynamics, the reduction in entropic gain that occurs when macromolecules dissolve in comparison to tiny molecules, makes native cellulose a macromolecule with a high dissolving

potential that is inherently difficult to dissolve. Additionally, cellulose has many hydroxyl groups. As seen in Figure 1, the hydroxyl groups' five oxygen atoms combine with ring- and bridge-oxygen to generate intricate patterns of hydrogen bonds. Lastly, cellulose has an amphiphilic character, meaning that the C and H atoms may interact through hydrophobic interactions. All in all, this places a great deal of demand on a cellulose solvent.

Derivatizing and non-derivatizing solvents are two categories of cellulose solvents based on whether the cellulose's molecular structure changes because of the solvents forming covalent bonds with it. Dimethylsulfoxide (DMSO) or N, N-dimethylformamide in combination with certain carboxylic acids, that is, CF3COOH, are examples of derivatizing solvents (Heinze & Koschella, 2005). Aqueous and nonaqueous media are the two categories into which non-derivatizing solvents can be separated; however, as many nonaqueous solvents contain some bound water in a salt or organic hydrate, this division is not always clear-cut (Olsson & Westman, 2013) for an extensive discussion on the direct dissolution of cellulose. Because cellulose dissolves differently in different solvents based on many factors, such as DP, purity, production process, and type of mixing, it is difficult to compare the dissolution capacity, the amount of dissolved cellulose per unit volume, of different solvents. Nonetheless, a systematic study in this area would be highly intriguing.

2.4.1 Aqueous media

Several water-based solvents are available, even though water cannot dissolve cellulose. These include low-temperature sodium hydroxide (NaOH) alone or combined with additives like polyethylene glycol, urea, and thiourea (Cai & Zhang, 2005; Isogai & Atalla, 1998; Yan & Gao, 2008; Zhang et al., 2002).

A different class of cellulose aqueous solvents comprises inorganic metal complexes, which are made up of nitrogen ligands and transition metal ions like cuprammonium hydroxide (Cuam), resulting in solutions with vibrant colors. Previous attempts to create fibers, artificial silk, with the Cuam solvent only reached a comparatively small-scale production due to the expensive cost of copper salts and the requirement to employ cotton cellulose. Melted inorganic salt hydrates and concentrated inorganic salt solutions, such as zinc chloride ($ZnCl_2*4H_2O$), lithium chloride ($LiCl*5H_2O$), magnesium chloride ($MgCl_2*6H_2O$), and lithium perchlorate ($LiClO_4*3H_2O$) are other examples of aqueous solvents (Fischer & Thümmler, 2010). Some of these have been helpful for homogeneous modification of cellulose.

Phosphoric acid, hydrochloric acid, and mixed acids can dissolve cellulose. However, when working with cellulose in acid, acid hydrolysis—which leads to chain degradation—is always a crucial consideration. A study by (Boerstoel et al., 2001) revealed some interesting findings: at room temperature, cellulose was quickly dissolved in anhydrous phosphoric acid to generate liquid crystalline solutions with a cellulose concentration of more than 7.5% (w/w). Airgap spinning with the cellulose solution in phosphoric acid (Northolt et al., 2001) was also used to create fibers. The fibers were then coagulated in acetone, rinsed with water, and neutralized with sodium carbonate. The mechanical parameters, first filament modulus of 44 GPa, strength of 1.7 GPa, outperformed the commercial fibers used as reference. It was demonstrated that the acid hydrolysis-related degradation in this instance was modest. Nevertheless, low strain-to-fail values were also produced by fibers with such high crystallinity (Röder et al., 2013).

2.4.2 Nonaqueous media

A typical nonaqueous solvent for cellulose is a mixture of N, N-dimethylacetamide (DMAc), and lithium chloride (LiCl). It is frequently used as reaction media for homogeneous modification of cellulose as well as for analytical characterization of polysaccharides (Dawsey & McCormick, 1990; Striegel, 1997). Although the solvent DMAc/LiCl is very effective, its sensitivity to water and other impurities makes industrial applications difficult, if not impossible, to use (Potthast et al., 2002; Rosenau et al., 2001). Additionally, an activation of the cellulose is required for its dissolution in DMAc/LiCl.

A further illustration of this kind of solvent is the tetrabutylammonium fluoride (TBAF*3H2O) and DMSO solution, which functions well since cellulose does not need to be activated. Thus far, it has been applied to laboratory-scale homogeneous chemical alteration of cellulose and analytical studies (Heinze & Köhler, 2010). Furthermore, cellulose does not require any preparation in DMAc or quaternary ammonium chlorides to dissolve it. As a result, by using this novel solvent, several of the drawbacks of DMAc/LiCl are avoided, including cellulose activation (Kostag et al., 2013). The discovery that cellulose dissolves fast even in an acetone/triethyloctylammonium chloride mixture with nine parts salt and twenty parts organic solvent is rather unexpected.

There is no need to activate or pretreat the cellulose. An additional increase in the concentration of triethyl octyl ammonium chloride does not negatively impact the solution. The 13C-NMR spectrum measured for cellulose dissolved in acetone/triethyl octyl ammonium chloride demonstrated that cellulose is not chemically modified during dissolution, that is, it is a non-derivatizing solvent. This has not yet been reported for binary acetone/salt mixtures,

including ionic liquids (ILs), where acetone has been found to cause immediate cellulose precipitation (Gericke et al., 2011).

2.4.2.1 N-methylmorpholine-N-oxide

N-methylmorpholine-N-oxide (NMMO) has been a commercially successful non-derivatizing solvent for cellulose. The Lyocell method, which creates cellulose textile fibers, is based on NMMO (Woodings, 1995). NMMO offers several benefits, including the ability to dissolve cellulose at high concentrations, the production of fibers with desirable mechanical characteristics (such as high wet and dry strength), and recycling nearly entirely after use (Fink et al., 2001; Woodings, 1995). NMMO is thermally unstable due to the N–O bond's high energy content, which is a significant disadvantage. Additionally, it is susceptible to catalytic impurities, which may cause unintended side effects (Rosenau et al., 2001; Wendler et al., 200; Wendler et al., 2008).

2.4.2.2 Ionic Liquids (ILs)

After the publication of a widely cited study by (Swatloski et al. in 2002) organic electrolytes with a melting point below 100°C, or ILs, became known for decades and became a new class of promising direct solvents for cellulose. Several in-depth review studies, such as (Cao et al., 2009; El Seoud et al., 2007; Isik et al., 2014; Pinkert et al., 2009;), have addressed ILs as cellulose solvents and their characteristics and interactions with cellulose. For ILs to be commercially successful, however, a few critical difficulties need to be further addressed, such as solvent recovery, side reactions, cellulose degradation, high solution viscosities that frequently call for the inclusion of another molecular solvent, and high viscosities (Gericke et al., 2012).

Figure 2. 5

Illustrates the Mechanism of Dissolution of Cellulose with Ionic Liquids

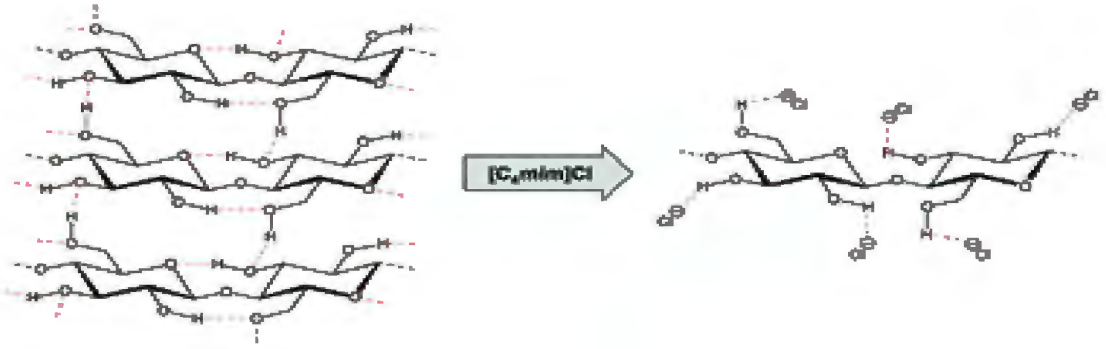

Figure 2. 6

Progress of the Dissolution of Cellulose (dissolving pulp) in 1-ethyl-3-methylimidazolium acetate (EMIMAc). (A) Solvent and starting material, (B) cellulose added into the solvent, (C) clear solution, (D) the starting material and the regenerated material. Reprinted with permission from Ref (Matyjaszewski & Möller, 2012). Copyright (2012) Elsevier

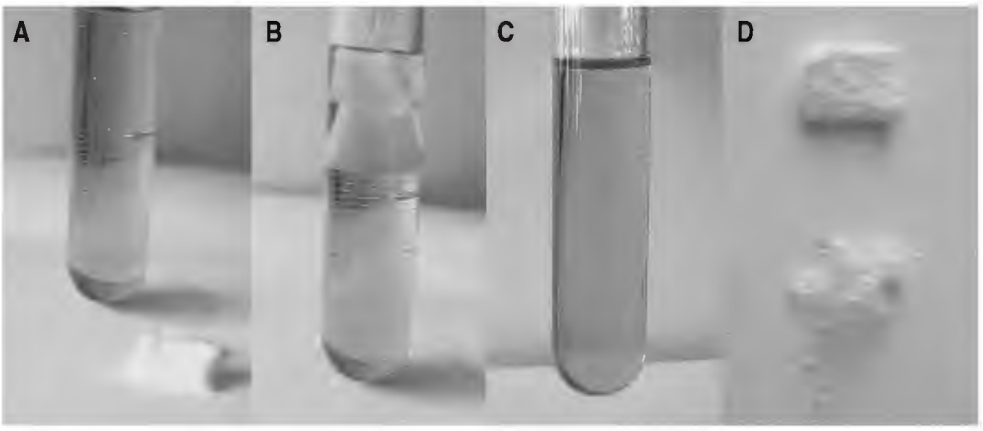

In a study published in 2012, Lv et al. examined the rheological characteristics of cellulose dissolved in 1-allyl-3-methylimidazolium chloride (AMIMCl) and 1-butyl-3-methylimidazolium chloride (BMIMCl), with DMSO acting as a co-solvent (Lv et al., 2012).

The results demonstrated that while the viscosities of the ILs were exponentially reduced upon the addition of DMSO, the cellulose structure remained unchanged, both in the entanglement and dilute regimes. At deficient cellulose concentrations, cellulose/IL/DMSO solutions behaved as Newtonian fluids. At more significant shear rates, the solution's viscosity displayed a shear-thinning characteristic as the concentration grew.

Research on imidazolium ions' thermostability revealed that ILs had a significantly lower propensity for degradation than NMMO (Wendler et al., 2012). Higher process temperatures with a decreased chance of exothermic reactions are made possible by the comparatively high decomposition temperatures of ILs, improving process safety. Nevertheless, it was shown that cellulose causes the endothermic breakdown of pure 1-ethyl-3-methylimidazolium acetate (EMIMAc) to change to an exothermic process.

2.5 Cellulose Modification

It is possible to create many cellulose derivatives by modifying the hydroxyl groups of cellulose, which are the reactive groups in the material (Matyjaszewski & Möller, 2012). Nucleophilic displacement reactions may also be used to modify cellulose chemically by forming deoxy derivatives of cellulose at the carbon atoms of the AGU (Heinze & Liebert, 2001). Also of ongoing interest is the oxidation of cellulose to introduce carboxyl or carbonyl groups (Heinze et al., 2012). Using different disintegration processes, cellulose could be a source of nano- and microscale materials. Accordingly, the cellulose's source, DP and crystallinity, and the treatment affect the nano- and microstructures' characteristics.

2.5.1 Cellulose Derivative

Research on the chemical modification of polysaccharides, such as cellulose, dates to the 1800s. For instance, the accidental discovery of cellulose's solubility in an acid mixture

(HNO_3/H_2SO_4) resulted in cellulose nitrate, one of the critical explosives of the Industrial Revolution (guncotton) (Bruma & Olabisi, 1997). Celluloid, the first synthetic plastic, was created by treating cellulose nitrate with camphor. Hyatt mentioned it in an early patent, whereby it was applied to billiard balls (Jedvert & Heinze, 2017). These days, cellulose acetate (CA), another cellulose ester, has greater significance than cellulose nitrate.

The commercial importance of typical carboxylic acid esters, such as CA, identified as early as 1865, is still enormous. Other notable polysaccharide esters include mixed acetate propionates, acetate butyrates, and acetate phthalates. The degree of substitution (DS) and the arrangement of the functional groups inside the repeating unit and along the polymer chains significantly impact the characteristics and solubility of CA(and nearly any other cellulose derivative. Applications for cellulose acetate and mixed cellulose carboxylic esters include films, membranes, and fibers (Fischer et al., 2008). Table 1 lists a few of the primary uses for cellulose esters. In sulfuric acid or perchloric acid as a catalyst, cellulose is converted with acetic acid and acetic anhydride to create CA in an industrial setting (Heinze, Liebert, & Koschella, 2006).

Table 2. 1

DP, Degree of Polymerization (Average Degree); DS, Degree of Substitution (Average Degree)

Cellulose ester	**DP**	**DS**		**Main application**
		Acetyl	**Propyl or butyl**	
Triacetate	150–360	2.8–3.0	–	Textile fibers, photo film, foil-insulating coatings

Cellulose ester	DP	DS		Main application
		Acetyl	Propyl or butyl	
Diacetate	100–200	2.5	–	Filter tow, thermoplastic mass
		2.4	–	Silk, foils, thermoplastic mass
Acetate/propionate	150–200	0.3	2.3	Thermoplastic mass
Acetate/butyrate	100–150	2.1	0.6	Raw materials for coating and insulation, foils
		2.0	0.7	Foils, films
		1.0	1.6	Thermoplastic mass
		0.5	2.3	Melt dipping mass

Aside from cellulose nitrate, CA, and the mixed carboxylic acid esters, cellulose sulfate (CS), another cellulose ester, has attracted some economic interest but has yet to be produced commercially. Recently, a unique and effective method for producing good water-soluble CS with high DS and DP was created (Gericke et al., 2009). The CS (Gericke et al., 2009; Wu et al., 2013) forms stable cationic complexes. Moreover, cellulose esters can be used in membrane technology, coatings, stationary phases in chromatography, and controlled release in the pharmaceutical industry. A wealth of fascinating research is being conducted on novel

esterification processes and cellulose products (Edgar, 2007; Matyjaszewski & Möller, 2012; Shanbhag et al., 2007).

The cellulose ethers, which include carboxymethyl cellulose (CMC), methylcellulose (MC), ethyl cellulose (EC), hydroxyethyl cellulose (HEC), hydroxypropyl cellulose (HPC), and mixed ethers (hydroxyethyl methylcellulose, HPMC, are another significant class of cellulose derivatives. These are all nontoxic and, as they are usually soluble in water, work well as thickeners, suspending agents, and flow-controlling agents. They are used in various sectors, such as paint, adhesives, food, medicine, and cosmetics (Feller & Wilt, 1991).

The field of cellulose modification into derivatives is vast, and many publications and reviews have been written about it, such as (Badshah et al., 2021; Habibi & Lucia, 2012; Kamide, 2005). This critical assessment will focus on cellulose derivatives, further explored in the "Cellulose shaping" section, which are used to shape materials like fibers and films.

2.5.2 Nanocellulose Materials

Various procedures can convert cellulose into materials at the micro- and nanoscale. In the years since, these materials have drawn a great deal of scientific study, see, for example, (Charreau et al., 2013; Klemm et al., 2011). The products undergo chemical, enzymatic, and mechanical shaping processes. Based on their characteristics, they are divided into several groups:

- microcrystalline cellulose (MCC),
- micro- or nanofibrillated cellulose (MFC/NFC), or cellulose nanofibrils (CNF)
- cellulose nanocrystals (CNC)/nanocrystalline cellulose (NCC), or whiskers, and
- bacterial nanocellulose (BNC).

A fine, white crystalline powder known as MCC is commercially made by treating cellulose with NaOH and then hydrolyzing it with acid. This powder has applications in food and paper as well as pharmaceuticals. Sub-structural fibrils are released during the preparation of MFC, which is accomplished by utilizing shear solid forces to break down wood pulp (Siró & Plackett, 2010). The heavily entangled fibrils form strong mechanical networks and gels.

Whiskers, also known as CNC/NCC, are cellulose particles that resemble stiff rods and are composed of smaller crystallites. Different methods can be used to prepare them, such as sonification and strong acid hydrolysis, although enzymatic treatments can produce particles with slightly different shapes. When included in composites, cellulose whiskers, and other nanocellulose materials have been demonstrated to produce outstanding results (Azizi Samir et al., 2005).

Water filtering membranes were the subject of a recent assessment of cellulose nanoparticles employed in environmental technology (Carpenter et al., 2015). Because cellulose is a cheap, renewable raw material with outstanding strength qualities, the scientists conclude that nanoparticles derived from it have considerable promise for various applications.

Nanoscale particles can also be produced from other cellulose derivatives, primarily esters, such as commercially available CAs, CA propionate, and CA butyrate, as well as from some organo-soluble cellulose ethers. Such particles can be produced using various techniques, including solvent evaporation during emulsification and dialysis-based solvent displacement (Hornig & Heinze, 2008). These particles can have a variety of uses, such as in the pharmaceutical and bioanalytics industries, depending on their functionalization (Schulze et al., 2016).

2.6 Cellulose Shaping

2.6.1 Textile Fibers

Nowadays, cotton provides most of the cellulose used to make textiles, making up more than 25% of the world's total fiber production (Möhl et al., 2022). Cotton production is recognized as unsustainable due to its high reliance on pesticides and considerable irrigation. As a result, there is a market for alternative fibers made, for example, from raw materials derived from wood. The Lyocell or viscose processes are two commercial methods for spinning fibers from dissolved cellulose. Because each of these processes has its own set of issues, research, and development are now being done on new solvents and spinning procedures.

2.6.1.1 Viscose

The term "viscose process" comes from the viscous cellulose solution used as spin dope, and it was initially reported by C. F. Cross, E. J. Bevan, and C. Beadle in the 1890s (Cross et al., 1893). In this procedure, carbon disulfide and sodium hydroxide react to transform cellulose into cellulose xanthogenate. Thus, one common cellulose derivative is the production of cellulose xanthogenate. Following its dissolution in aqueous sodium hydroxide, cellulose xanthogenate is employed in a wet-spinning procedure in which the cellulose solution precipitates as pure cellulose fibers in an acidic coagulation bath, primarily sulfuric acid with a wide range of other components, including salts. The technique produces high-performance fibers and is still commonly utilized. Regrettably, the process has several drawbacks, including environmental concerns related to the use of sulfuric reagents, wastes, and heavy metals in the regeneration baths. Figure 5 shows the spinning of the viscose fibers.

Figure 2. 7

The Spinning of Viscose Fibers through a Spinneret, reprinted with permission Ref (Heinze & Liebert, 2001) … copyright (2012) Elsevier

2.6.1.2 Lyocell

Cellulose staple fibers are produced commercially using the Lyocell method using NMMO as the solvent. This process has many advantages and is widely accepted for usage in nonwoven and textile applications (Fink et al., 2001). Nonetheless, an ongoing study is carried out because of the solvent-related issues that were previously noted, such as NMMO's thermal instability and the interaction of NMMO with water, as shown in Refs. (Perepelkin, 2007; Biganska & Navard, 2005). The degree of these issues can be prevented, for example, by using stabilizers in the solutions.

2.6.1.3 Noncommercial Processes

2.6.1.3.1 aqueous alkali

Cellulose dissolving in aqueous alkali, either with or without previous derivatization, is the basis of several noncommercial procedures. The process of carbamate formation, which is cellulose reacting with urea to generate cellulose carbamate, is identical to the viscose process (Sixta et al., 2015). After that, cellulose carbamate can be treated similarly to cellulose xanthate (Fu et al., 2014) without releasing hazardous substances. The lack of appropriate fiber characteristics is probably why the process has not been commercialized.

Another cellulose derivative that dissolves in aqueous alkali is cellulose carbonate. Oh, et al. (Oh et al., 2002) proposed a method in which cellulose is treated with carbon dioxide at low temperatures to produce ethyl acetate, for example. Zinc oxide (ZnO) can be added as an additive, and the cellulose carbonate can be dissolved in a sodium hydroxide solution. Wet spinning using acidic coagulation baths can produce fibers. Nevertheless, the strength of the fibers was slightly less than that of reference rayon fibers, and they frequently displayed skin features (Oh et al., 2005).

Numerous researchers have investigated fiber spinning from cellulose solutions in NaOH without first derivatizing. Early research was conducted by (Kamide et al., 1984), who used spectroscopic techniques to study the dissolution of pre-treated cellulose in NaOH. Fiber spinning experiments were conducted to continue the study, wherein cellulose soaked in NaOH was wet spun into acidic coagulation baths. In contrast to commercially regenerated fibers, the fiber's qualities were noticeably inferior (Yamashiki et al., 1992). The addition of chemicals to the NaOH solution has resulted in improved fiber characteristics and cellulose solubility.

2.6.1.3.2 Ionic Liquids

Many researchers have examined the use of ILs in manufacturing cellulose dope and fiber spinning, a topic that was recently the subject of a comprehensive literature review (Hummel et al., 2016). Common ILs, including BMIMCl, 1-ethyl-3-methylimidazolium chloride (EMIMCl), and EMIMAc, were compared with cellulose dissolving in NMMO in a (Kosan et al., 2008) study. Dry-wet spinning was used to form the cellulose dopes. The viscosities of the ILs' cellulose solutions were equivalent to those of comparable fibers spun from NMMO monohydrate.

However, they could still be molded into fibers with noticeably greater tenacities (see Figure 7). The same research group also investigated the feasibility of using ILs to manufacture CA fibers. Before dry-wet spinning to fibers, cellulose dissolved in IL was allowed to react with varying molar ratios of acetic anhydride to AGU to control the DS. The ratio of acetic anhydride to cellulose affected the fiber's characteristics; a larger ratio produced a higher DS and decreased tenacity, in both the conditioned and wet states, in comparison to the cellulose fiber, which was not altered.

Figure 2.8

Products (fibers, yarns, and knitted fiber) made from Cellulose in EMIMAc. Reproduced with Permission from Thuringian Institute of Textile and Plastics Research. For more examples, Sec Ref. (Hermanutz, Gähr, Uerdingen, Meister, & Kosan, 2008)

The use of ILs to produce cellulose textile fibers has also seen some intriguing recent breakthroughs (Sixta et al., 2015). The IL 1,5-diazabicyclo [4.3.0]non-5-enium acetate ([DBNH][OAc]), a superbase and direct solvent for cellulose, is the basis of the proposed process (dubbed Ioncell-F). Strong fibers with tenacities continuously exceeding 50 cN/tex have been generated from cellulose solutions containing 15%–17% cellulose using airgap spinning. However, further work on developing a solvent recycling system is required to bring the technology to market.

3 MATERIALS AND METHODS

D (+)-Cellobiose, EC 208-436-5 from Man. Sigma Aldrich Slovakia was used as received without any modifications. Sodium Citrate was purchased from Matheson Coleman and Bell Manufacturing Chemist, Norwood, Ohio, U.S.A. Sodium carbonate, sodium bicarbonate, and sodium iodide were purchased from Mallinckrodt Baker, Inc., Paris, Kentucky. Sodium sulfite, sodium phosphate, sodium bromide, and sodium nitrite were purchased from Fair Lawn, New Jersey, U.S.A. We acquired sodium chloride and sodium sulfate from E.M.D. Chemicals Inc. in Gibbstown, New Jersey, U.S.A., and Darmstadt, Germany. Sodium borate and sodium formate were purchased from J.T. Baker Chemical Co. Philipsburg. New Jersey U.S.A. Sodium azide, sodium oxalate, sodium nitrate, and sodium fluoride were purchased from Tower Drug and Chemical Company in Rochester, New York, and Across Organics, New Jersey, U.S.A., respectively. D7 A.T.R. and electric weighing scale were purchased from Thermos Fisher Scientific U.S.A. and Sargent-Welch V.W.R. Scientific, respectively. Other materials include laboratory pistons and mortar, Viars, desiccators, and TGA instruments.

3.1 Sample preparation

0.1mmol (0.0342g) of cellobiose was weighed using the electric scale. Also, 0.1 mmol of each sodium salt was weighed out, and the two compounds (cellobiose + each sodium salt) were mixed with an agate mortar and pestle for 2.0 min to give a homogeneous sample. 0.1mmol (0.0342g) of cellobiose was weighed out and kept in a vial. The mixtures are kept in a vial and allowed to dry in a Drierite (8 mesh) desiccator for three days.

3.2 Characterization

3.2.1 Spectroscopic technique

The cellobiose and the mixture, cellobiose and sodium salt, spectra were recorded once using D7 ATR. The pure cellobiose peaks were read relative to each of the mixtures (cellobiose + sodium salts). That is, the pure cellobiose spectrum was used as a reference to obtain the difference (peak shift in each of the sodium salt spectra.

Figure 3. 1

FTIR Instrument

3.2.2 Thermogravimetric Analysis (TGA)

About 5 mg portion of the mixtures were transferred to the platinum crucible, and the TG curve was recorded at 25–800°C in the air using a heating rate of 10 grad/min. A pure cellobiose TGA curve was also recorded under similar conditions. The peak area ratios of pure

cellobiose and each cellobiose salt were calculated. Peak area ratios of pure cellobiose were used as a reference or as a control for the cellobiose-salt mixtures.

Figure 3. 2

Thermogravimetric analyzer

3.2.3 Computational Method

D-cellobiose, a cellulose model compound with two D-glucose units, was the subject of a computational study. It existed as two anomers, α and β, and both anomers were considered. Figure 8 displays the geometries of the α and β D-cellobiose anomers as well as the four potentials up- and down-face approaches of sodium chloride. The structures were drawn using the GuassView 6.0 program and then sent to Gaussian 09W for optimization and the creation of computational clusters. Density Functional Theory (DFT) computations utilizing the B3LYP

exchange-correlation function approach were used for these structural modifications. (Yu et al., 2022; People et al., 1992; Stephens et al., 1994). The basis set 6-31+g^1 with polarization functions for each atom was applied (Montgomery Jr et al., 1999; Montgomery Jr et al., 2000). The charge distributions of the atoms were analyzed using the Mulliken population analysis. The distance, bond length in Å, between each oxygen atom on the cellobiose and sodium ions of the salts was calculated and tabulated considering Å≤ 3.5 Binding energies (Hf) of the D-cellobiose-sodium salts complex were calculated and the free binding energies were obtained using the equation shown below:

$E_{free(Hf)}$ =(Energy of the complex) – (I.E.C + I.E.Ss).

4 RESULTS AND DISCUSSION

The quest for chemical modification of polymers for various applications has been the order of the day. Research has been done to find a suitable group(s) of compounds that will have a degree of modification of cellulose. When utilized in unaltered forms like cotton or wood, cellulose is on a lesser scale in specific applications like regenerated fibers, for example, viscous or paper industry. Moreover, cellulose can be modified chemically, enzymatically, or microbiologically to produce new, valuable derivatives and materials. Numerous significant industrial sectors, including the paint, polymer, and membrane industries, use large-scale manufacture of cellulose derivatives and regenerated materials (Klemm, Heublein, Fink, & Bohn, 2005). Chemical modification of cellulose was performed by adding sodium salts, and the interactions were characterized by using three methods.

4.1 Spectroscopic Analysis Result

Figure 4. 1

IR Spectrum of D-Cellobiose

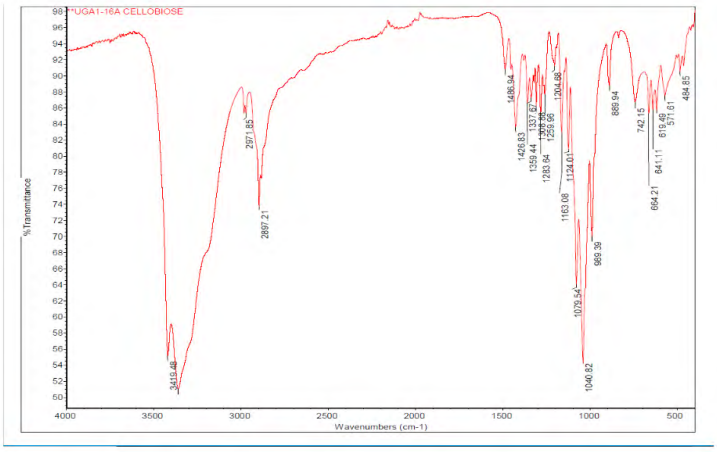

Figure 4. 2

The IR spectrum of sodium carbonate and D-cellobiose Mixture

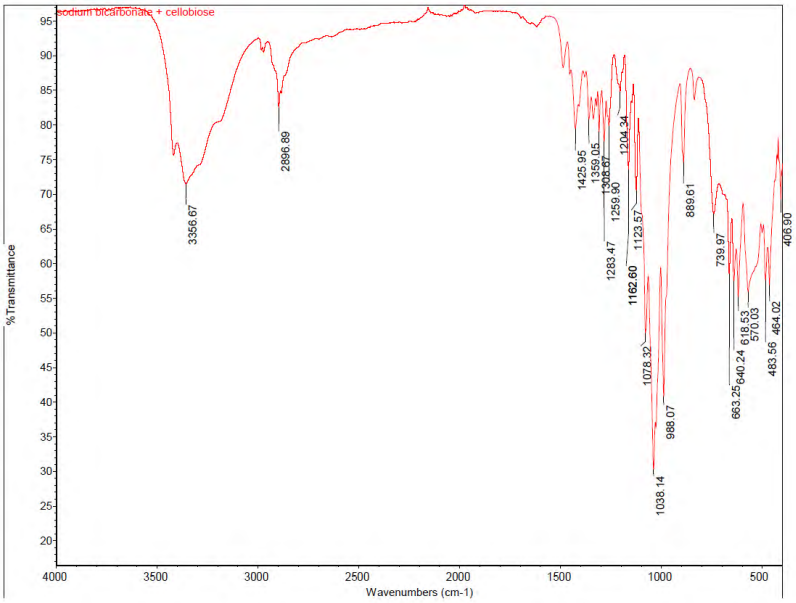

Table 4. 1

shows the peak shift of the cellobiose-sodium salts mixture as regards pure cellobiose

Cellobiose	3360.28	2897.21	1426.83	1359.44	1283.64	1163.08	1124.01	1079.54	1040.82	989.39	Σpeak shift
NaN_3 + cellobiose	3355.84(-4.44)	2896.96(-0.25)	1426.13(-0.7)	1359.04(-0.4)	1283.41(-0.23)	1162.59(-0.52)	1123.49(-0.52)	1078.39(-1.15)	1038.31(-2.51)	988.12(-1.12)	13.99
$NaHCO_3$ +Cellobiose	3356.69(-3.61)	2896.89(-0.32)	1425.95(-0.88)	1359.05(-0.39)	1283.47(-0.17)	1162.60(-0.48)	1123.57(-0.44)	1078.32(-1.22)	1038.14(-2.68)	988.07(-1.32)	11.51
Na_2B4O_7+Cellobiose	3349.09(-11.19)	2896.99(-0.22)	1425.37(-1.46)	1337.89(-21.55)	1258.47(-24.9)	1162.32(-0.76)	1127.00(+2.99)	1078.36(-1.18)	1038.15(-2.67)	988.48(-0.91)	40.03
Na_3C6H5O_7 +Cellobiose	3358.31(-1.97)	2896.98(-0.23)	1421.41(-5.42)	1360.21(+0.77)	1282.19(-1.45)	1161.59(-1.49)	1123.79(-0.22)	1078.37(-1.17)	1039.08(-1.74)	988.57(-0.82)	13.74
NaHCOO +Cellobiose	3355.79(-4.49)	2896.29(-0.92)	1424.65(-2.18)	1359.54(+0.10)	1282.54(-1.10)	1162.29(-0.79)	1123.09(-0.92)	1076.04(-3.50)	1037.83(-2.99)	987.46(-1.93)	18.72
$NaNO_3$ +Cellobiose	3358.17(-2.11)	2896.50(-0.71)	1431.15(+4.32)	1357.22(-2.22)	1283.23(-0.41)	1162.42(-0.66)	1123.14(-0.87)	1078.07(-1.47)	1038.28(-2.54)	987.96(-1.43)	7.77
$NaNO_2$ +Cellobiose	3358.51(-1.77)	2896.47(-0.88)	1425.99(-0.84)	1358.95(-0.49)	1282.83(-0.81)	1162.45(-0.63)	1123.14(-0.87)	1077.81(-1.73)	1038.01(-2.81)	987.93(-1.46)	12.29
Na_2C2O_4 +Cellobiose	3354.95(-5.33)	2896.33(-0.88)	1417.95(-8.88)	1358.97(-0.47)	1283.64(-0.02)	1162.62(-0.46)	1123.30(-0.71)	1078.28(-1.26)	1038.56(-2.26)	988.25(-1.14)	22.67
$Na_3(PO4)_2$ +Cellobiose	3360.56(+0.28)	2896.89(-0.32)	1426.22(-0.61)	1359.17(-0.27)	1259.73(-23.91)	1162.41(-0.67)	1122.73(-1.18)	1074.93(-4.61	1039.52(-1.30)	988.46(-0.93)	33.42
Na_2SO_4 +Cellobiose	3358.65(-1.63)	2896.96(-0.25)	1426.08(-0.75)	1359.11(-0.33)	1283.47(-0.17)	1161.90(-1.18)	1123.13(-0.88)	1078.32(-1.22)	1038.16(-2.66)	988.13(-1.26)	10.33
Na_2SO_3 +Cellobiose	3358.95(-1.38)	2896.85(-0.36)	1426.02(-0.81)	1359.08(-0.36)	1283.44(-0.20)	1162.62(-0.46)	1123.46(-0.55)	1078.60(-0.94	1038.53(-2.29)	987.83(-1.56)	8.91
Na_2CO_3 +Cellobiose	3357.77(-2.51)	2898.82(-0.39)	1426.26(-0.57)	1359.09(-0.35)	1283.40(-0.24)	1162.59(-0.49)	1123.51(-0.50)	1078.44(-1.10)	1038.43(-2.39)	988.18(-1.21)	9.75
NaF + Cellobiose	3355.51(-4.47)	2896.64(-0.57)	1425.41(-1.07)	1358.76(-0.68)	1283.06(-0.58)	1162.30(-0.78)	1123.23(-0.78)	1075.96(-3.58)	1037.25(-3.57)	987.43(-1.96)	18.04
NaCl +Cellobiose	3359.65(-0.63)	2896.39(-0.82)	1426.79(-0.04)	1359.33(-0.11)	1259.85(-23.79)	1162.59(-0.49)	1123.56(-0.45)	1078.30(-1.24)	1038.17(-2.65)	988.01(-1.38)	31.6
NaBr +Cellobiose	3361.23(+0.95)	2896.06(-1.15)	1425.24(-1.59)	1359.60(+0.16)	1282.91(-0.73)	1162.45(-0.63)	1123.09(0.92)	1077.32(-2.22	1037.68(-3.14)	987.64(-1.75)	11.02
NaI +Cellobiose	3353.13(-7.15)	2896..63(-0.58)	1425.11(-1.72)	1358.80(-0.64)	1282.91(-0.73)	1161.76(-1.32)	1122.60(-1.41)	1073.41(-6.13)	1036.97(-3.85)	987.04(-1.08)	24.61

Firstly, the spectroscopic technique (FT-IR) depicts the spectrum of the pure and cellobiose mixture. From the spectrum, it was observed that there is a 50% transmittance at the O-H region of the cellobiose. The addition of sodium salt to the cellobiose altered the transmittance value. There was also a slight change in the distinct peaks compared with the cellobiose. The result showed that the mixtures of cellobiose + sodium nitrate and cellobiose + sodium borate had the lowest and highest peak shifts of 77 cm^{-1}, and 40.037 cm^{-1} respectively, compared with the peaks of pure cellobiose.

4.2 Thermogravimetric Analysis (TGA)

Figure 4. 3

Shows the TGA/DTA Curve of Cellobiose

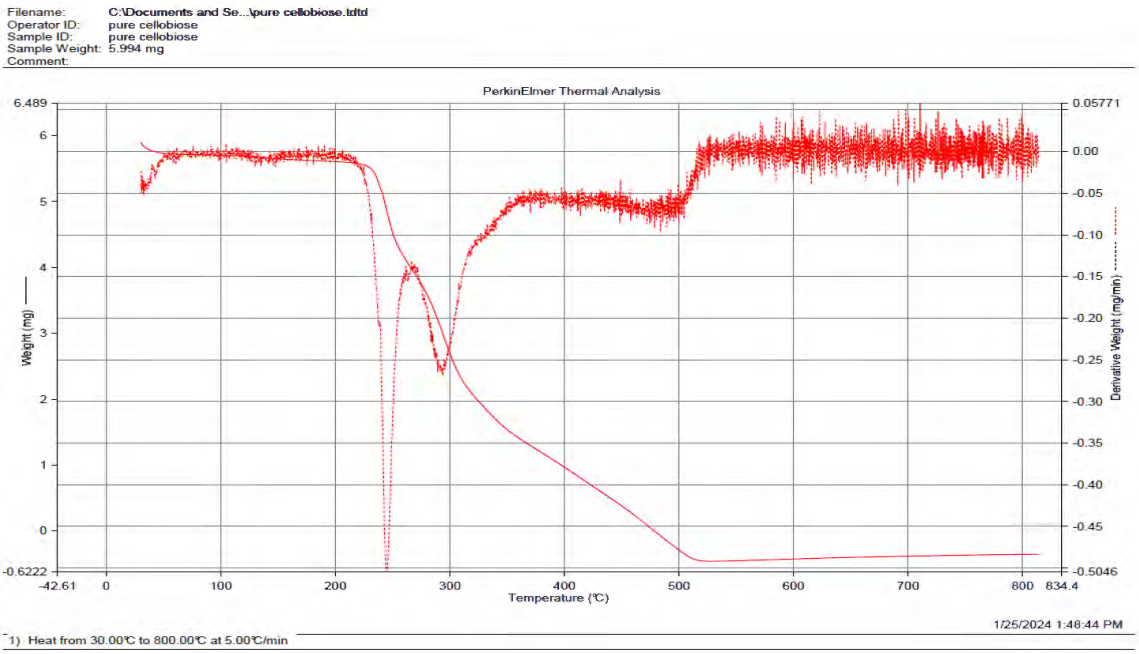

Figure 4. 4

Shows the TGA/DTA of the Cellobiose+ Sodium Azide Mixture

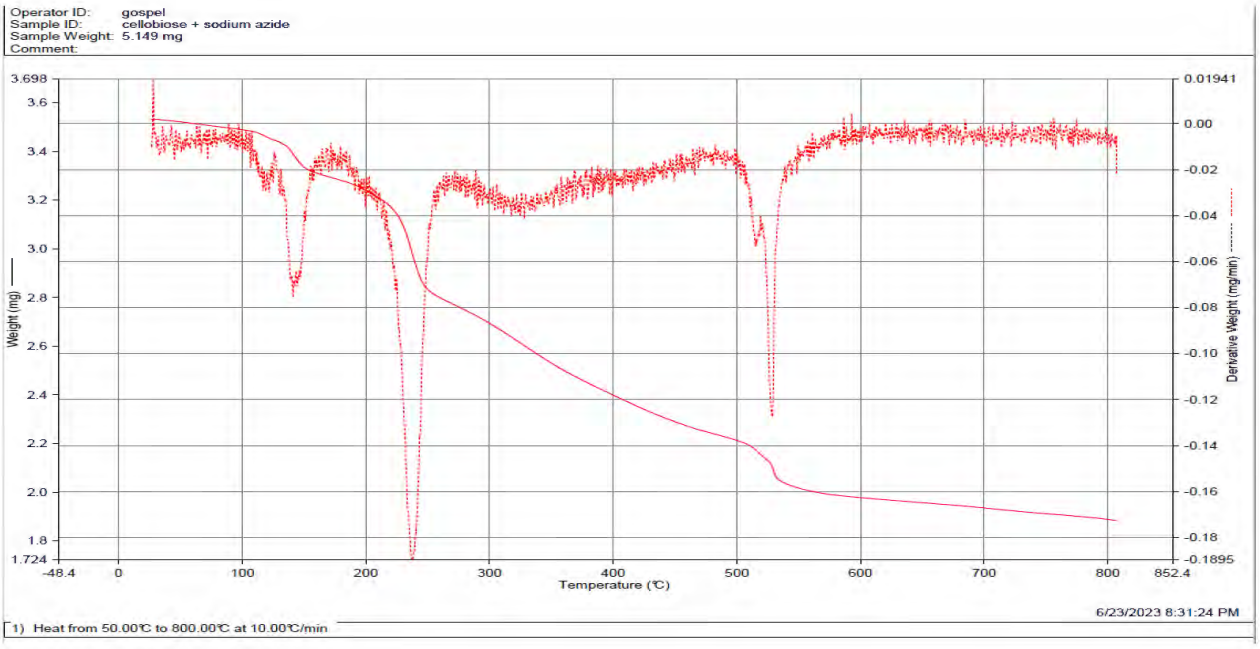

Secondly, thermogravimetric analysis was used to elucidate the stability, decomposition rates, high and low volatility, and combustion temperatures of cellobiose and sodium salt mixtures. The result showed a decomposition of highly volatile compounds for cellobiose at 245 °c, low volatile compounds at 295 °c, and a combustion temperature of 500 °c. Adding sodium salt to the cellobiose example, cellobiose + sodium citrate changed the decomposition and combustion temperature to 212 °c, 280 °c, and 620 °c, respectively.

Many cellobiose-salt mixtures showed little or no significant low volatility decomposition temperature, that is, they changed directly from the decomposition of highly volatile compounds to combustion. Halogen mixtures showed an identical decomposition pattern on high volatility decomposition temperature of 225 °c, no significant low volatility decomposition temperature, and a slight difference in the combustion temperature with sodium

chloride and sodium bromide at 525 °c (+25 °c), and sodium fluoride at 580 °c (+80 °c). Some sodium salts like carbonate, sulfate, citrate, formate, and bicarbonate increase the combustion temperature and, thus, enhance the stability of cellobiose with temperature with cellobiose + sodium carbonate having the highest combustion temperature of 700 °c (+200 °c) compared to pure cellobiose of 500 °c combustion temperature. Some sodium salts, such as sulfate and phosphate, with combustion temperatures of 472 °c (-28 °c) and 480 °c (-20 °c), respectively, reduce the combustion temperature, thus making cellobiose combust at a lower temperature.

Table 4. 2

Shows the Samples' Peak Area Ratios

Samples	*Peak area ratio (A)*	*(B)*	*(C)*	*(D)*
D-Cellobiose	*1.77*	*2.04*	*1.36*	*N/A*
Cellobiose + NaN_3	*0.40*	*0.61*	*0.19*	*N/A*
Cellobiose + $NaHCO_3$	*0.88*	*0.80*	*0.57*	*N/A*
Cellobiose + Na_3BO_3	*0.95*	*1.11*	*0.36*	*N/A*
Cellobiose + $Na_2C_6H_50_7$	*1.16*	*1.01*	*2.02*	*N/A*
Cellobiose + Na_2CO_3	*0.25*	*0.40*	*0.16*	*N/A*
Cellobiose + $NaNO_3$	*0.84*	*0.62*	*0.30*	*N/A*
Cellobiose + $NaNO_2$	*1.22*	*0.74*	*0.44*	*N/A*

Cellobiose + $Na_2C_2O_4$	*1.27*	*0.85*	*0.70*	*N/A*
Cellobiose + Na_3HPO4	*0.07*	*0.76*	*N/A*	*N/A*
Cellobiose + Na_2SO_4	*1.49*	*0.68*	*0.88*	*N/A*
Cellobiose + Na_2SO_3	*0.80*	*1.22*	*N/A*	*N/A*
Cellobiose + NaHCOOH	*2.10*	*0.90*	*0.30*	*N/A*
Cellobiose + NaBr	*1.53*	*1.41*	*0.78*	*0.47*
Cellobiose + NaCl	*1.79*	*0.84*	*0.73*	*N/A*
Cellobiose + NaF	*2.20*	*1.00*	*0.70*	*N/A*
Cellobiose + NaI	*1.65*	*0.85*	*1.05*	*N/A*

Table 4. 3

Shows the Degradation and Combustion Temperatures of Cellobiose and Cellobiose-Sodium Salts Mixtures

samples	Temp. at high volatility (℃)	Temp. at low volatility (℃)	Combustion temp. (℃)
Cellobiose	245	295	500
Cellobiose + Na_2SO_4	250 (+5)	295 (0)	472 (-25)
Cellobiose + Na_3HPO4	225 (-20)	N/A	480 (-20)
Cellobiose + Na_2C_2O4	245 (0)	295 (0)	520 (+20)
Cellobiose + $NaNO_3$	245 (0)	N/A	520 (+20)
Cellobiose + NaN_3	245 (0)	350 (+ 55)	520 (+20)
Cellobiose + NaBr	225 (-20)	N/A	525 (+25)
Cellobiose + NaCl	225 (-20)	N/A	525 (+25)
Cellobiose + NaF	225 (-20)	N/A	580 (+80)
Cellobiose + NaI	225 (-20)	N/A	545 (+45)
Cellobiose + Na_3BO_3	245 (0)	N/A	530 (+30)

Cellobiose + $NaNO_2$	180 (-65)	N/A	530 (+30)
Cellobiose + $NaHCO_3$	180 (-65)	N/A	600 (+100)
Cellobiose + NaHCOOH	200 (-45)	N/A	600 (+100)
Cellobiose + $Na_2C_6H_50_7$	212 (-33)	280 (-55)	620 (+120)
Cellobiose + Na_2SO_3	210 (-35)	N/A	650 (+150)
Cellobiose + Na_2CO_3	180 (-65)	N/A	700(+200)

4.3 Computational method

Figure 4. 5

The up and down Approach of Sodium Chloride towards Cellulose Model Anomers: α and β D-Cellobiose

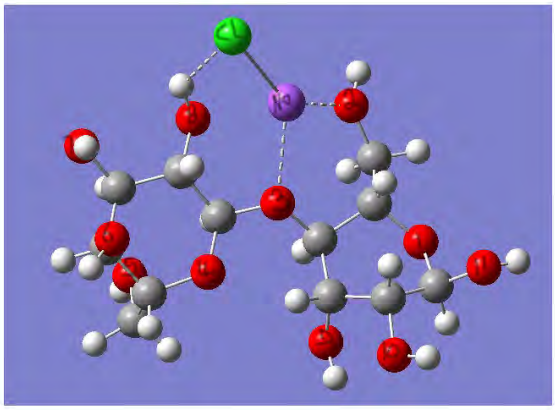

D-Cellobiose (α) + Sodium Chloride-Up

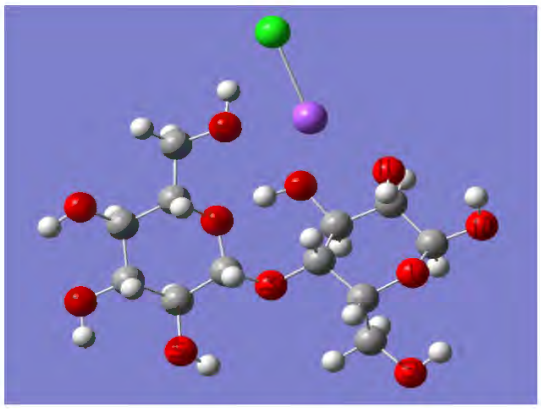

D-Cellobiose (β) + Sodium Chloride-Up

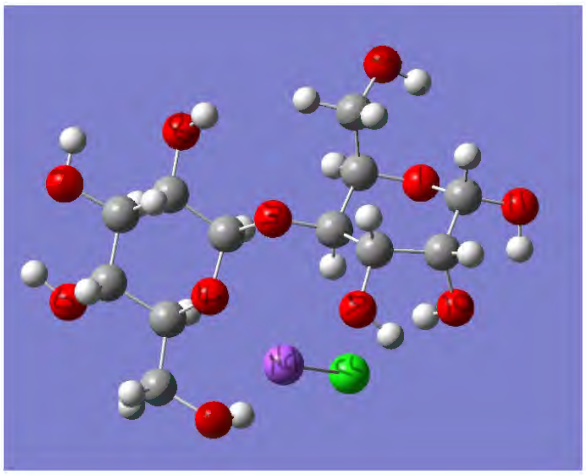

D-Cellobiose (α) + Sodium Chloride-Down

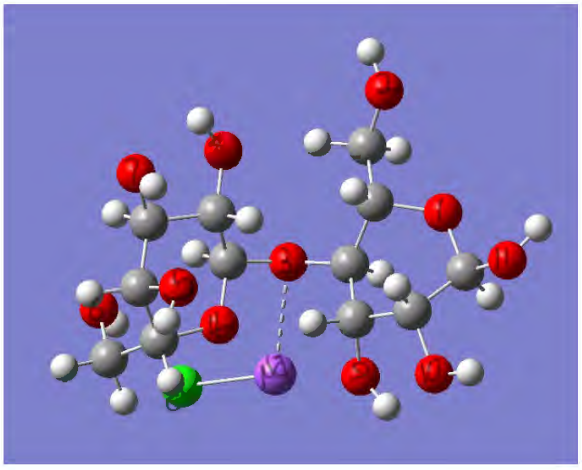

D-cellobiose (β) +Sodium Chloride-Down

Lastly, computational studies showed that the reaction between α-cellobiose and sodium nitrite at the down approach had the lowest total reaction energy of -97 KCal/mol and the highest was between sodium borate at the up approach and β-cellobiose with an energy of 30.88 Kcal/mol. The up face of α-cellobiose with halogens showed similar interacting behavior with the salts interacting to the same OH position of 2,3 and 8 in the cellobiose-optimized structure. Sodium fluoride had its shortest bond length of 2.233 Å in position 8. In comparison, 2.237 Å and 2.205 Å were the shortest bond lengths of sodium chloride and sodium bromide, respectively, and in position 2. Sodium Borate had the shortest bond length of 1.708 Å in the 8th OH position of α- cellobiose up face position and 1.708 Å in the position 4 OH. Sodium nitrite and sodium nitrate had one binding position of 2.188 Å and 2.231 Å, respectively, at OH position 2 of α-cellobiose up face. Sodium azide (NaN_3) showed the shortest bond length of 1.882 Å position 10 of the OH group of α-cellobiose down the face. Halogens also showed similar interaction patterns to the OH of the α-cellobiose down face on positions 3,4, and 9, respectively. Sodium fluoride had the shortest bond length of 2.211 Å at position four, while Sodium chloride and sodium bromide were in position 9 of the OH.

Table 4. 4

Shows the Calculation Summary of the D-Cellulose, Sodium Chloride, and Cellobiose-Sodium Chloride Mixture

G1:M1:V1 - Gaussian Calculation Summary

Overview | Thermo | Opt

Alpha cellobiose-OPT		
C:/Users/kahuna/Desktop/opt files/Alpha cell...		
File Type	.chk	
Calculation Type	FOPT	
Calculation Method	RB3LYP	
Basis Set	6-31+G	
Charge	0	
Spin	Singlet	
Solvation	None	
Electronic Energy	-1297.546904	Hartree
RMS Gradient Norm	0.000007	Hartree/Bohr
Imaginary Freq		
Dipole Moment	5.836686	Debye
Point Group		

G1:M1:V1 - Gaussian Calculation Summary

Overview | Thermo | Opt

Sodium chloride-OPT		
C:/Users/kahuna/Desktop/opt files/Sodium ...		
File Type	.chk	
Calculation Type	FOPT	
Calculation Method	RB3LYP	
Basis Set	6-31G	
Charge	0	
Spin	Singlet	
Solvation	None	
Electronic Energy	-622.550765	Hartree
RMS Gradient Norm	0.000000	Hartree/Bohr
Imaginary Freq		
Dipole Moment	9.203308	Debye
Point Group		

G1:M1:V1 - Gaussian Calculation Summary

Overview | Thermo | Opt

Alpha cellobiose-OPT + sodium chloride- OPT		
C:/Users/kahuna/Desktop/opt files/Alpha cell...		
File Type	.chk	
Calculation Type	FOPT	
Calculation Method	RB3LYP	
Basis Set	6-31+G	
Charge	0	
Spin	Singlet	
Solvation	None	
Electronic Energy	-1920.161068	Hartree
RMS Gradient Norm	0.000006	Hartree/Bohr
Imaginary Freq		
Dipole Moment	14.044124	Debye
Point Group		

Table 4. 5

Bond Lengths between Monosodium Ions of the Salts and Oxygens on the Cellobiose

Bond length α-Cellobiose (Å)	O1-Na	O2-Na	O3-Na	O4-Na	O5-Na	O6-Na	O7-Na	O8-Na	O9-Na	O1O-Na	O11-Na	Energy (KCal/Mol
NaN_3 (U)	4.769	2.243	2.423	4.446	5.700	5.917	5.017	2.285	5.841	6.450	5.656	-36.17
$NaHCO_3$ (U)	8.096	6.569	5.017	5.448	5.512	4.754	2.294	2.369	8.336	9.629	9.917	-34.86
NaHCOOH (U)	4.858	2.248	2.453	4.370	5.952	5.619	4.808	2.282	5.889	6.631	6.176	-12.70
$NaNO_3$ (U)	4.021	2.231	4.747	5.926	7.902	8.151	4.718	5.360	6.230	5.721	4.792	-83.51
$NaNO_2$ (U)	4.861	2.188	5.275	7.393	8.504	8.320	7.238	4.670	7.530	8.077	6.226	-92.88
NaF (U)	4.788	3.794	2.408	4.457	5.800	5.894	4.682	2.233	5.826	6.337	5.737	-64.60
NaCl (U)	4.800	2.237	2.396	4.390	5.963	5.564	4.955	2.327	5.822	6.523	6.054	-39.78
NaBr (U)	5.006	2.205	2.712	4.360	6.101	4.560	4.962	2.220	5.741	7.138	6.798	-65.20
NaN_3 (D)	5.227	7.630	4.964	4.432	6.193	7.073	8.641	7.611	3.359	1.882	4.666	-16.75
$NaHCO_3$ (D)	7.763	10.066	7.455	6.481	5.803	9.049	9.892	9.054	4.758	6.505	8.836	-9.64
NaHCOO (D)	5.681	8.342	5.968	5.515	7.754	7.688	9.573	8.665	3.605	2.398	5.079	-8.95
$NaNO_3$ (D)	3.700	5.873	4.640	5.365	4.872	8.217	8.013	5.954	2.232	4.778	5.554	-69.09
$NaNO_2$ (D)	4.828	7.627	5.489	5.341	6.827	8.183	9.518	8.147	2.325	2.251	4.846	-97.94
NaF (D)	5.110	6.761	2.712	2.211	4.244	5.099	6.378	5.318	2.307	4.736	6.509	-42.26
NaCl (D)	5.368	6.713	2.481	2.394	4.027	5.415	6.470	5.200	2.317	4.868	6.627	-35.74
NaBr (D)	4.874	6.436	2.406	2.328	4.404	5.273	6.436	5.111	2.311	4.941	6.477	-51.53
Bond length β-Cellobiose (Å)												Energy (KCal/Mol
NaF (U)	2.341	3.644	4.389	3.302	6.781	7.320	6.127	2.346	5.073	4.746	3.266	-65.33
NaCl (U)	4.968	2.336	4.681	3.639	7.125	7.624	6.361	3.427	7.389	5.222	2.479	-59.29
NaBr (U)	4.960	2.278	2.510	4.370	6.845	6.540	4.908	2.234	5.321	6.541	7.065	-36.85
NaN_3 (U)	5.711	2.286	3.197	2.324	5.662	6.432	5.560	2.325	7.207	6.763	4.456	-71.60
$NaHCO_3$ (U)	2.348	5.251	4.363	3.362	6.669	7.349	6.061	2.286	4.541	3.614	3.996	25.16
NaHCOO (U)	5.175	2.432	3.413	2.433	5.796	6.567	5.609	2.293	7.052	6.285	3.999	-20.39
$NaNO_3$ (U)	5.015	2.354	4.068	3.077	6.118	6.875	5.672	-8.95	7.220	5.665	3.045	-57.73
$NaNO_2$ (U)	5.015	7.220	4.068	3.077	2.362	5.672	6.875	6.118	2.354	3.045	5.665	-48.30
NaF (D)	4.996	6.944	3.354	2.366	2.300	5.521	6.481	5.680	2.380	3.594	5.914	-22.48
NaCl (D)	5.256	7.033	3.211	2.315	2.316	5.568	6.394	5.663	2.318	3.993	6.335	-6.39
NaBr (D)	5.234	7.026	3.218	2.318	2.323	5.568	6.403	5.666	2.320	3.985	6.318	-59.46
NaN_3 (D)	5.355	5.018	2.429	4.425	2.323	5.093	6.692	6.903	2.393	5.080	6.563	-73.37
$NaHCO_3$ (D)	5.170	3.984	2.433	2.310	2.327	4.958	6.794	7.189	4.903	6.510	5.943	-26.04
$NaNO_2$ (D)	5.431	2.325	2.390	3.741	3.938	5.592	6.685	6.187	6.153	6.613	5.017	-31.95
$NaNO_3$ (D)	5.424	2.737	2.358	4.462	2.404	5.084	6.865	7.169	5.795	6.697	5.373	-48.12
NaHCOO (D)	5.467	2.325	2.391	3.880	3.815	5.585	6.770	6.303	6.099	6.617	4.908	-27.68

Table 4. 6

Bond Lengths Between Di and Trisodium Ions of the Salts and Oxygens on the Cellobiose

Bond length α-Cellobiose (Å)						Energy (KCal/mol
Na_2CO_3	(U)	O7-Na1 (2.314)	O8-Na1 (2.946)			-50.70
$Na_2C_2O_4$	(U)	O1-Na1 (3.101)	O2-Na1 (2.475)			-13.08
Na_2HPO_4	(U)	O2-Na1 (2.157)				-21.47
Na_2SO_4	(U)	O2-Na1 (2.439)	O2-Na2 (2.407)	O3-Na2 (3.170)	O8-Na2 (2.208)	-93.35
Na_2SO_3	(U)	O3-Na1 (3.206)	O8-Na1 (2.228)	O2-Na2 (2.267)		-50.70
Na_3BO_3	(U)	O2-Na1 (2.276)	O4-Na2 (1.780)			11.18
$Na_3C_6H5O_7$	(U)					-7.51

Bond length α-Cellobiose (Å)							Energy (KCal/mol
Na_2CO_3	(D)	O3-Na1 (3.300)	O4-Na1 (2.192)	O9-Na1 (3.500)	O9-Na2 (3.256)	O10-Na2-(2.351)	-31.26
$Na_2C_2O_4$	(D)	O5-Na1 (2.787)	O10-Na2 (2.249)				-30.22
Na_2HPO_4	(D)	O9-Na1 (2.527)	O10-Na1 (2.433)				12.02
Na_2SO_4	(D)	O9-Na1 (3.466)	O10-Na1 (2.432)				-79.11
Na_2SO_3	(D)	O3-Na1 (3.500)	O4-Na1 (2.288)	O9-Na1 (2.291)			-30.29
Na_3BO_3	(D)	O3-Na1 (3.027)	O4-Na1 (1.780)	O9-Na2 (2.276)			25.26
$Na_3C_6H5O_7$	(D)	O9-Na1 (3.366)	O10-Na1 (2.271)				-22.78

Bond length β-Cellobiose (Å)						Energy (KCal/mol
Na_2CO_3	(U)	O2-Na1 (2.295)	O8-Na1 (2.486)			-57.28
$Na_2C_2O_4$	(U)	O1-Na1 (2.360)	O8-Na1 (2.390)			-60.45
Na_2HPO_4	(U)	O1-Na1 (2.379)	O3-Na1 (2.921)	O8-Na1 (2.285)	O8-Na2 (2.316)	-59.75
Na_2SO_4	(U)	O8-Na1 (2.294)	O2-Na2 (2.304)	O11-Na2 (2.342)		-85.14
Na_2SO_3	(U)	O2-Na1 (2.281)	O8-Na1 (3.376)	O7-Na2 (2.414)	O8-Na2 (2.445)	-54.08
Na_3BO_3	(U)	O2-Na1 (1.829)	O3-Na1 (2.902)	O8-Na1 (2.271)		30.88
$Na_3C_6H_5O_7$	(U)					-95.35

Bond length β-Cellobiose (Å)						Energy (KCal/mol
Na_2CO_3	(D)	O1-Na1- (2.314)	O11-Na1 (2.534)	O5-Na2 (2.236)		-50.06
$Na_2C_2O_4$	(D)	O2-Na1 (2.357)	O3-Na1 (2.623)	O4-Na1 (2.463)		-61.61
Na_2HPO_4	(D)	O8-Na1 (2.323)	O9-Na1 (2.337)			-52.63
Na_2SO_4	(D)	O5-Na1 (2.391)	O9-Na2 (2.338)			-83.86
Na_2SO_3	(D)	O1-Na1 (2.372)	O10-Na1 (2.370)	O11-Na1 (2.705)	O5-Na2 (2.274)	-87.9
Na_3BO_3	(D)					12.23
$Na_3C_6H5O_7$	(D)					-62.64

Generally, most sodium salts on the up face have closer interaction with the OH of α-cellobiose at 2,3 and 8 positions, with positions 2 and 3 having the highest number, while in the down face, the most positions of interaction with the sodium salt were at 3,4, and 9 with 9 having the highest number of interactions. On the other hand, sodium salts interact with β-cellobiose at 2,4 and 8 OH groups of the cellulose model when the salts approach from up with OH at position 8 having the most significant number of interactions. Unlike α-cellobiose, β-cellobiose has some interaction with some salts, such as, sodium fluoride and sodium chloride, at OH position 11 from the up approach.

Halogens have a dissimilar interaction pattern when they approach β-cellobiose from the up with sodium chloride and sodium bromide interacting with OH at 2 position, fluoride, and chloride sodium salts at position 11. When the sodium salts approach β-cellobiose from the down, most salts have their interaction with the OH at 4 and 5, while halogens interact at position 11, and all salts show a binding behavior on OH at 3. Considering both the up and down approach of the salts to the β-cellobiose, it was observed that OH at position 3 had the highest interactions with the sodium salts.

Table 4. 7

Shows the Number of Interactions Between Sodium Salts (up) and α-Cellobiose

O positions in α-cellobiose (U)	no of interaction
O1	1
O2	12
O3	7
O4	0
O5	0
O6	0
O7	2
O8	9
O9	0
O10	0
O11	1

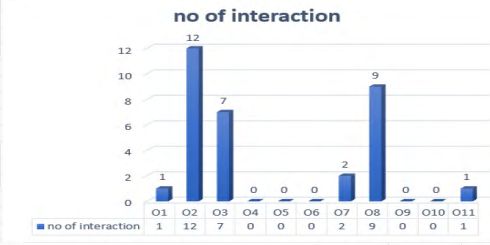

no of interaction between sodium salts (up) and α-cellobiose

Table 4. 8

shows the interactions between sodium salts (D) and α-cellobiose

O position in α-cellobiose (D)	no of interaction
O1	0
O2	0
O3	3
O4	3
O5	0
O6	0
O7	0
O8	0
O9	6
O10	3
O11	0

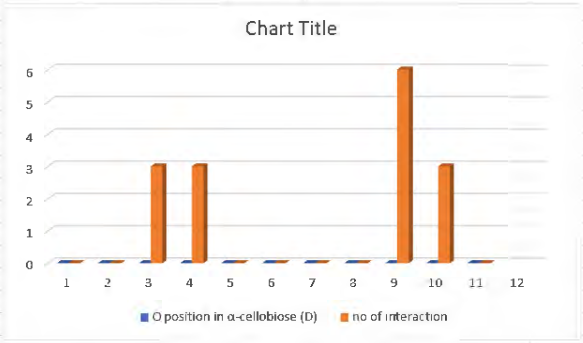

interaction between sodium salts (D) and α-cellobiose

Table 4. 9

shows the energies between α D- $C_{12}H_{12}O_{11}$ and sodium salts (up)

Energy of α D-$C_{12}H_{22}O_{11}$ and sodium Salts (UP)	Energy of the compex	Individual Energy	I.E.C +I.E.Ss	Binding Energy (Hf)	Energy (KCal/mol
Alpha cellobiose		-1297.546904			
Alpha cellobiose + NaN_3	-1623.950199	-326.345661	-1623.892565	-0.057634	-36.17
Alpha cellobiose + $NaHCO_3$	-1724.28319	-426.680735	-1724.227639	-0.055551	-34.86
Alpha cellobiose +NaBr	-4031.598380	-2733.947568	-4031.494472	-0.103908	-65.20
Alpha cellobiose +Na_2CO_3	-1886.043718	-588.435363	-1885.982267	-0.061451	-38.56
Alpha cellobiose + NaCl	-1920.161068	-622.550765	-1920.097669	-0.063399	-39.78
Alpha cellobiose + $Na_3C_6H_5O_7$	-2542.755521	-1245.196648	-2542.743552	-0.011969	-7.51
Alpha cellobiose + NaF	-1559.7928	-262.142943	-1559.689847	-0.102953	-64.60
Alpha cellobiose + HCOONa	-1649.084323	-249.6607167	-1649.060263	-0.0202406	-12.70
Alpha cellobiose + $NaNO_3$	-1740.117305	-440.067519	-1739.98423	-0.133075	-83.51
Alpha cellobiose + $NaNO_2$	-1664.978522	-410.283592	-1664.830496	-0.148026	-92.88
Alpha cellobiose +$Na_2C_2O_4$	-1998.201301	-697.733547	-1998.180451	-0.02085	-13.08
Alpha cellobiose + Na_2HPO_4	-2265.052524	-967.471404	-2265.018308	-0.034216	-21.47
Alpha cellobiose + Na_2SO_4	-2321.112306	-1023.416638	-2320.963542	-0.148764	-93.35
Alpha cellobiose + Na_2SO_3	-2246.019828	-948.392137	-2245.939041	-0.080787	-50.70
Alpha cellobiose + Na_3BO_3	-2035.17875	-737.649664	-2035.196568	0.017818	11.18
Free binding energy = (energy of the complex) - (I.E.C + I.E. Ss)					
		1 Hatfree =627.5095 Kcal/mol			
I.E.C = Individual energy of the cellobiose					
I.E.Ss =Individual energy of the salts					

Table 4. 10

shows the energies between α D- $C_{12}H_{12}O_{11}$ and sodium salts (down)

Energy of α D-$C_{12}H_{22}O_{11}$ and sodium Salts (DOWN)	Energy of the compex	Individual Energy	I.E.C +I.E.Ss	Binding Energy (Hf)	Energy (KCal/mol
Alpha cellobiose		-1297.546904			
Alpha cellobiose + NaN_3	-1623.919257	-326.345661	-1623.892565	-0.026692	-16.75
Alpha cellobiose + $NaHCO_3$	-1724.243008	-426.680735	-1724.227639	-0.015369	-9.64
Alpha cellobiose +NaBr	-4031.576585	-2733.947568	-4031.494472	-0.082113	-51.53
Alpha cellobiose +Na_2CO_3	-1886.03208	-588.435363	-1885.982267	-0.049813	-31.26
Alpha cellobiose + NaCl	-1920.154626	-622.550765	-1920.097669	-0.056957	-35.74
Alpha cellobiose + $Na_3C_6H_5O_7$	-2542.779849	-1245.196648	-2542.743552	-0.036297	-22.78
Alpha cellobiose + NaF	-1559.757193	-262.142943	-1559.689847	-0.067346	-42.26
Alpha cellobiose + HCOONa	-1649.024518	-349.513359	-1649.010263	-0.014255	-8.95
Alpha cellobiose + $NaNO_3$	-1740.151791	-442.367526	-1739.914423	-0.110095	-69.09
Alpha cellobiose + $NaNO_2$	-1664.986577	-365.283592	-1664.830496	-0.156081	-97.94
Alpha cellobiose +$Na_2C_2O_4$	-1999.328605	-697.733547	-1999.280451	-0.048154	-30.22
Alpha cellobiose + Na_2HPO_4	-2264.999145	-967.471404	-2265.018308	0.019163	12.02
Alpha cellobiose + Na_2SO_4	-2321.089617	-1023.416638	-2320.963542	-0.126075	-79.11
Alpha cellobiose + Na_2SO_3	-2245.987303	-948.392137	-2245.939041	-0.048262	-30.29
Alpha cellobiose + Na_3BO_3	-2035.156306	-737.649664	-2035.196568	0.040262	25.26
Free binding energy = (energy of the complex) - (I.E.C + I.E. Ss)					
I.E.C = Individual energy of the cellobiose		1 Hatfree =627.5095 Kcal/mol			
I.E.Ss =Individual energy of the salts					

4. 11 Table

Shows the Energies Between β D- $C_{12}H_{12}O_{11}$ and Sodium Salts (up)

Energy of β D-$C_{12}H_{22}O_{11}$ and sodium Salts (UP)	Energy of the compex	Individual Energy	I.E.C +I.E.Ss	Binding Energy (Hf)	Energy (KCal/mol
Beta cellobiose		-1297.551888			
Beta cellobiose + NaN_3	-1624.00895	-326.345661	-1623.897541	-0.11409	-71.60
Beta cellobiose + $NaHCO_3$	-1724.19254	-426.680735	-1724.232623	0.04009	25.16
Beta cellobiose +NaBr	-4031.558200	-2733.947568	-4031.49948	-0.05872	-36.85
Beta cellobiose +Na_2CO_3	-1886.07853	-588.435363	-1885.987243	-0.091287	-57.28
Beta cellobiose + NaCl	-1920.19746	-622.550765	-1920.102653	-0.094807	-59.29
Beta cellobiose + $Na_3C_6H_5O_7$	-2542.900489	-1245.196648	-2542.748536	-0.151953	-95.35
Beta cellobiose + NaF	-1559.798945	-262.142943	-1559.694831	-0.1041105	-65.33
Beta cellobiose + HCOONa	-1647.09774	-349.513359	-1647.065247	-0.032493	-20.39
Beta cellobiose + $NaNO_3$	-1737.711405	-440.067519	-1737.619407	-0.0919982	-57.73
Beta cellobiose + $NaNO_2$	-1662.912454	-365.283592	-1662.83548	-0.076974	-48.30
Beta cellobiose +$Na_2C_2O_4$	-1995.381772	-697.733547	-1995.285435	-0.096337	-60.45
Beta cellobiose + Na_2HPO_4	-2265.118502	-967.471404	-2265.023292	-0.09521	-59.75
Beta cellobiose + Na_2SO_4	-2321.10421	-1023.416638	-2320.968526	-0.135684	-85.14
Beta cellobiose + Na_2SO_3	-2246.030221	-948.392137	-2245.944025	-0.086196	-54.08
Beta cellobiose + Na_3BO_3	-2035.152342	-737.649664	-2035.201552	0.04921	30.88
Free binding energy = (energy of the complex) - (I.E.C + I.E. Ss)					
I.E.C = Individual energy of the cellobiose		1 Hatfree =627.5095 Kcal/mol			
I.E.Ss =Individual energy of the salts					

Table 4. 12

Shows the Energies Between β D- $C_{12}H_{12}O_{11}$ and Sodium Salts (down)

Energy of β D-$C_{12}H_{22}O_{11}$ and sodium Salts (DOWN)	Energy of the compex	Individual Energy	I.E.C +I.E.Ss	Binding Energy (Hf)	Energy (KCal/mol
Beta cellobiose		-1297.551888			
Beta cellobiose + NaN_3	-1624.014469	-326.345661	-1623.897541	-0.116928	-73.37
Beta cellobiose + $NaHCO_3$	-1724.274121	-426.680735	-1724.232623	-0.041498	-26.04
Beta cellobiose +NaBr	-4031.594240	-2733.947568	-4031.49948	-0.09476	-59.46
Beta cellobiose +Na_2CO_3	-1886.067015	-588.435363	-1885.987243	-0.079772	-50.06
Beta cellobiose + NaCl	-1920.112838	-622.550765	-1920.102653	-0.010185	-6.39
Beta cellobiose + $Na_3C_6H_5O_7$	-2542.64871	-1245.196648	-2542.748536	-0.099826	-62.64
Beta cellobiose + NaF	-1559.730649	-262.142943	-1559.694831	-0.035818	-22.48
Beta cellobiose + HCOONa	-1647.109364	-349.513359	-1647.065247	-0.044117	-27.68
Beta cellobiose + $NaNO_3$	-1737.696095	-440.067519	-1737.619407	-0.076688	-48.12
Beta cellobiose + $NaNO_2$	-1662.886398	-365.283592	-1662.83548	-0.050918	-31.95
Beta cellobiose +$Na_2C_2O_4$	-1999.78361	-697.733547	-1995.285435	-0.098175	-61.61
Beta cellobiose + Na_2HPO_4	-2265.607157	-967.471404	-2265.023292	-0.083865	-52.63
Beta cellobiose + Na_2SO_4	-2321.602206	-1023.416638	-2320.968526	-0.13368	-83.86
Beta cellobiose + Na_2SO_3	-2246.084109	-948.392137	-2245.944025	-0.140084	-87.9
Beta cellobiose + Na_3BO_3	-2035.182004	-737.649664	-2035.201552	0.019548	12.23
Free binding energy = (energy of the complex) - (I.E.C + I.E. Ss)					
I.E.C = Individual energy of the cellobiose		1 Hatfree =627.5095 Kcal/mol			
I.E.Ss =Individual energy of the salts					

In conclusion, although both anomers of D-cellobiose had slight differences in the interactions with the selected sodium salts on both approaches, up and down, the OH group at positions 2 and 3 had the most interactions with the sodium salts. Sodium citrate in up approach with α-cellobiose showed no strong interactions, that is, each of the sodium ions of the salts with the OH groups of the cellobiose had a bond length that is more than 3.5Å, and this could be because of the bulky nature of sodium citrate compared to other salt samples.

Table 4. 13

Shows the Individual Salts and their Corresponding Parameters

sample																
NaF												*	*	*	*	*
NaCl												*	*	*		*
NaBr											*	*	*	*		*
NaI																
NaN_3													*		*	
$NaHCO_3$			*													
NaHCOOH													*		*	
$NaNO_3$		*						*							*	
$NaNO_2$			*												*	
Na_2CO_3			*		*											
Na_2SO_4				*		*										
Na_2SO_3							*									
Na_2C2O_4																
Na_2HPO_4																
Na_3BO_3	*								*	*	*					
$Na_3C_6H_5O_7$																
	Highest IR Peak shift	lowest IR Peak shift	lowest temp. of high volatile compound	Highest temp. of high volatile compound	Highest combustion temp.	Lowest combustion temp.	Highest total energy	Lowest total energy	Shortest bond length α-D Up	Shortest bond length α-D Down	Shortest bond length β-D Up	Shortest bond length β-D Down	Highest no of salt interaction with α-cellobiose up	Highest no of salt interaction with α-cellobiose Down	Highest no of salt interaction with β-cellulose up	Highest no of salt interaction with β-cellulose Down

5 CONCLUSIONS

The addition of sodium salt to cellobiose showed how cellobiose interacts with each of the salts. Characterizing this modified cellobiose behavior showed that incorporating sodium borate (Na3BO3) into cellobiose had more effect in peak shift on the IR spectrum compared to pure cellobiose having a peak shift of (δ) of 40.03 cm^{-1} followed by sodium phosphate (Na_2HPO_4) with a δ= 33.42 cm^{-1} The minor peak shifts were observed in sodium nitrate (NaNO3) and sodium sulfite (NaNO2) with δ of 7.77 cm^{-1} and 8.91 cm^{-1}, respectively. The highest peak shifted when the salts were introduced in the cellobiose had more effect on the OH group of the cellobiose as observed in the IR spectrum. Na_3BO_3 has a negative free reaction energy of -4.558 kJ/mol and has more affinity with the cellulose material which may be the reason why boron-containing fillers are widely employed as a flame-retardant additive, in a variety of cellulosic-based materials from diverse sources, including paper, fabric, sawdust, insulating material, and timber. (Ali et al.,2019; Marney & Russell, 2008; Yuksel et al., 2014).

It is also observed that the decomposition temperature of pure cellobiose was altered because of chemical modification with the sodium salt, as seen in the thermogram of the TGA analyzer. Most salts like sodium sulfate and sodium phosphate reduce the temperature at which cellobiose decomposes, i.e., making it less stable with an increase in temperature, while salts like sodium carbonate, sodium sulfite, and sodium citrate increase the decomposition temperature of cellobiose therefore, making it more stable to high heat. Two often utilized minerals that are both very effective at gas-phase flame retardancy and kind to the environment are $CaCO_3$ and Na_2CO_3. By thermally decomposing, it absorbs some of the heat and emits CO_2,

which lowers the quantity of oxygen in the flame and combustible volatiles. (Gilman, 2013; Jimoh et al., 2018; Morgan)

The computational method gave insight into the geometries and electronic structure of the molecule to understand the electronic energies, the total energy, and bond length between the sodium ion (Na+) in the sodium salts and OH groups in the cellobiose. Most monosodium salts like NaN_3 NaHCOO, NaF, NaCl, and NaBr interact more with the α- cellobiose when the salt approaches from the up position at 2,3 and 8. When these salts approached from the downside of the cellobiose, they made their interaction at positions 3,4 and 9.

From this simulation technique, halogens had similar binding positions and almost the same bond lengths. The binding energies between the cellobiose and each sodium salt were calculated. From the result, cellobiose-sodium sulfite had the least total binding energy of -183.690kj/mol, while cellobiose-sodium sulfite had the highest total binding energy of 1207.021kj/mol. The mixture, cellobiose-sodium salt with a negative total binding energy indicated that the individual salt + cellobiose energy is more significant than the energy of the complex molecule (when reacted together). In contrast, that with positive total binding energy implies that the energy of the complex is greater than the individual salt + cellobiose energy.

5.1. Future work: Since sodium salts have been used to characterize cellobiose thermal, spectroscopic, and computational behavior, it would be worthwhile to consider metal ions like lithium and potassium salts, which are more electropositive than sodium, to know the most efficient metal that would be used in cellobiose chemical modification.

REFERENCES

Alban, S., & Franz, G. (2000). Characterization of the anticoagulant actions of a semisynthetic curdlan sulfate. *Thrombosis Research, 99(5),* 377-388.

Azizi Samir, M. A. S., Alloin, F., & Dufresne, A. (2005). Review of recent research into cellulosic whiskers, their properties, and their application in nanocomposite field. *Biomacromolecules, 6(2),* 612-626.

Badshah, M., Ullah, H., Wahid, F., & Khan, T. (2021). Properties and applications of modified bacterial cellulose-based materials. *Current Nanoscience, 17(3),* 351-364.

Biganska, O., & Navard, P. (2005). Kinetics of precipitation of cellulose from cellulose− NMMO− water solutions. *Biomacromolecules, 6(4),* 1948-1953.

Boerstoel, H., Maatman, H., Westerink, J., & Koenders, B. (2001). Liquid crystalline solutions of cellulose in phosphoric acid. *Polymer, 42(17),* 7371-7379.

Bruma, M., & Olabisi, O. (1997). *Handbook of thermoplastics*. O Olabisi, Dekker N. Y., 771-798.

Burton, B. A., & Brant, D. A. (1983). Comparative flexibility, extension, and conformation of some simple polysaccharide chains. Biopolymers: *Original Research on Biomolecules, 22(12),* 1769-1792.

Cai, J., & Zhang, L. (2005). Rapid dissolution of cellulose in LiOH/urea and NaOH/urea aqueous solutions. *Macromolecular Bioscience, 5(6),* 539-548.

Cao, Y., et al. (2009). Room temperature ionic liquids (RTILs): A new and versatile platform for cellulose processing and derivatization. *Chemical Engineering Journal, 147(1),* 13-21.

Carpenter, A. W., de Lannoy, C.-F., & Wiesner, M. R. (2015). Cellulose nanomaterials in water treatment technologies. *Environmental Science & Technology, 49(9),* 5277-5287.

Charreau, H., Foresti, M. L., & Vazquez, A. (2013). Nanocellulose patents trends: A comprehensive review on patents on cellulose nanocrystals, microfibrillated and bacterial cellulose. *Recent Patents on Nanotechnology, 7(1),* 56-80.

Chen, Y., et al. (2014). Acetylation and carboxymethylation of the polysaccharide from Ganoderma atrum and their antioxidant and immunomodulating activities. *Food Chemistry, 156,* 279-288.

Cross, C., Bevan, E., & Beadle, C. (1893). Thiokohlensäureester der cellulose. *Berichte der Deutschen Chemischen Gesellschaft, 26,* 1090-1097.

Dawsey, T., & McCormick, C. L. (1990). The lithium chloride/dimethylacetamide solvent for cellulose: a literature review. *Journal of Macromolecular Science, Part C: Macromolecular Chemistry and Physics, 30(3-4),* 405-440.

De France, K. J., Hoare, T., & Cranston, E. D. (2017). Review of hydrogels and aerogels containing nanocellulose. *Chemistry of Materials, 29(10),* 4609-4631.

Dufresne, A. (2012). Potential of nanocellulose as a reinforcing phase for polymers. *Journal of Science and Technology for Forest Products and Processes, 2(1),* 6-16.

Edgar, K. J. (2007). Cellulose esters in drug delivery. *Cellulose, 14(1),* 49-64.

El Seoud, O. A., Koschella, A., Fidale, L. C., Dorn, S., & Heinze, T. (2007). Applications of ionic liquids in carbohydrate chemistry: a window of opportunities. *Biomacromolecules, 8(9),* 2629-2647.

Feller, R. L., & Wilt, M. H. (1991). *Evaluation of cellulose ethers for conservation*. Getty Publications.

Fink, H., & Philipp, B. (1985). Models of cellulose physical structure from the viewpoint of the cellulose I→ II transition. *Journal of Applied Polymer Science, 30(11),* 3779-3790.

Fink, H., Ganster, J., Fraatz, J., & Nywlt, M. (1994). Relations between structure and mechanical properties of cellulosic man-made fibres. In.

Fink, H.-P., Hofmann, D., & Philipp, B. (1995). Some aspects of lateral chain order in cellulosics from X-ray scattering. *Cellulose, 2(1),* 51-70.

Fink, H.-P., Weigel, P., Purz, H., & Ganster, J. (2001). Structure formation of regenerated cellulose materials from NMMO-solutions. *Progress in Polymer Science, 26(9)*, 1473-1524.

Fischer, S., & Thümmler, K. (2010). Molten inorganic salts as reaction medium for cellulose. in Cellulose Solvents: For Analysis, Shaping and Chemical Modification *(pp. 91-101). ACS Publications.*

Fischer, S., et al. (2008). *Properties and applications of cellulose acetate*. Wiley Online Library, *Vol. 262*, 89-96.

Fu, F., et al. (2014). Green method for production of cellulose multifilament from cellulose carbamate on a pilot scale. *ACS Sustainable Chemistry & Engineering, 2(10),* 2363-2370.

Gao, G., Jiao, Q., & Li, X. (2005). Structural modification of pachymaran and the mechanism interaction between Azur A. *Acta Laser Biology Sinica, 14(3),* 228.

Goebel, W. F., & Adams, M. H. (1943). The immunological properties of the heterophile antigen and somatic polysaccharide of pneumococcus. *Journal of Experimental Medicine, 77(5),* 435.

Gericke, M., Fardim, P., & Heinze, T. (2012). Ionic liquids—promising but challenging solvents for homogeneous derivatization of cellulose. *Molecules, 17(6),* 7458-7502.

Gericke, M., Liebert, T., & Heinze, T. (2009). Interaction of ionic liquids with polysaccharides, 8—synthesis of cellulose sulfates suitable for polyelectrolyte complex formation. *Macromolecular Bioscience, 9(4),* 343-353.

Gericke, M., Liebert, T., & Heinze, T. (2009). Polyelectrolyte synthesis and in situ complex formation in ionic liquids. *Journal of the American Chemical Society, 131(38),* 13220-13221.

Gu, B., & Doner, H. E. (1992). *The interaction of polysaccharides with Silver Hill illite*. Clays and Clay Minerals, *40(1),* 151-156.

Habibi, Y., & Lucia, L. A. (2012*). Polysaccharide building blocks*: A sustainable approach to the development of renewable biomaterials. John Wiley & Sons.

Hattori, K., et al. (1998). Synthesis of sulfonated amino-polysaccharides having anti-HIV and blood anticoagulant activities. *Carbohydrate Research, 312(1-2),* 1-8.

Hattori, M., Koga, T., Shimaya, Y., & Saito, M. (1998). Aqueous calcium thiocyanate solution as a cellulose solvent. Structure and interactions with cellulose. *Polymer Journal, 30(1),* 43-48.

Hattori, M., Shimaya, Y., & Saito, M. (1998). Structural changes in wood pulp treated by 55 wt% aqueous calcium thiocyanate solution. *Polymer Journal, 30(1),* 37-42.

Heinze, T. (1998). New ionic polymers by cellulose functionalization. *Macromolecular Chemistry and Physics, 199(12),* 2341-2364.

Heinze, T., & Koschella, A. (2005). Solvents applied in the field of cellulose chemistry: a mini review. *Polímeros, 15(1),* 84-90.

Heinze, T., & Liebert, T. (2001). Unconventional methods in cellulose functionalization. Progress in *Polymer Science, 26(9),* 1689-1762.

Heinze, T., & Köhler, S. (2010). Dimethyl sulfoxide and ammonium fluorides—novel cellulose solvents. in Cellulose Solvents: For Analysis, Shaping and Chemical Modification (pp. 103-118). *ACS Publications*.

Heinze, T., Koschella, A., Liebert, T., Harabagiu, V., & Coseri, S. (2012). Cellulose: Chemistry of cellulose derivatization. *European Polysaccharide Network of Excellence (EPNOE) Research Initiatives & Results,* 283-327.

Heinze, T., Liebert, T., & Koschella, A. (2006). *Esterification of polysaccharides*. Springer Science & Business Media.

Henriksson, M., & Berglund, L. A. (2007). Structure and properties of cellulose nanocomposite films containing melamine formaldehyde. *Journal of Applied Polymer Science, 106(6),* 2817-2824.

Hermanutz, F., Gähr, F., Uerdingen, E., Meister, F., & Kosan, B. (2008). *New developments in dissolving and processing of cellulose in ionic liquids. In Cellulose Solvents*: For Analysis, Shaping and Chemical Modification (*Vol. 262*, pp. 23-27). Wiley Online Library.

Hornig, S., & Heinze, T. (2008). Efficient approach to design stable water-dispersible nanoparticles of hydrophobic cellulose esters. *Biomacromolecules, 9(4),* 1487-1492.

Hummel, M., et al. (2016). Ionic liquids to produce man-made cellulosic fibers: opportunities and challenges. In Cellulose Chemistry and Properties: *Fibers, Nanocelluloses and Advanced Materials* (pp. 133-168). *Springer International Publishing*.

Isik, M., Sardon, H., & Mecerreyes, D. (2014). Ionic liquids and cellulose: dissolution, chemical modification, and preparation of new cellulosic materials. *International Journal of Molecular Sciences, 15(7),* 11922-11940.

Isobe, N., et al. (2013). TEMPO-oxidized cellulose hydrogel as a high-capacity and reusable heavy metal ion adsorbent. *Journal of Hazardous Materials, 260,* 195-201.

Isogai, A., & Atalla, R. (1998). Dissolution of cellulose in aqueous NaOH solutions. *Cellulose, 5(4),* 309-319.

Jedvert, K., & Heinze, T. (2017). Cellulose modification and shaping—a review. *Journal of Polymer Engineering, 37(9),* 845-860.

Jimoh, O. A., Ariffin, K. S., Hussin, H. B., Temitope, A. E. (2018). Synthesis of precipitated calcium carbonate: *A review. Carbonates and Evaporites, 33(2),* 331–346.
(17) (PDF) Flame Retardant Material Based on Cellulose Scaffold Mineralized by Calcium Carbonate.

Kamida, K., Okajima, K., Matsui, T., & Kowsaka, K. (1984). Study on the solubility of cellulose in aqueous alkali solution by deuteration IR and 13C NMR. *Polymer Journal, 16(11),* 857-866.

Kamide, K. (2005). *Cellulose and cellulose derivatives*. Elsevier.

Klemm, D., et al. (2011). Nanocelluloses: A new family of nature-based materials. *Angewandte Chemie International Edition, 50(24),* 5438-5466.

Klemm, D., Heublein, B., Fink, H., & Bohn, A. (2005). Cellulose: fascinating biopolymer and sustainable raw material. *Angewandte Chemie International Edition, 44(22),* 3358-3393.

Klemm, D., Philpp, B., Heinze, T., Heinze, U., & Wagenknecht, W. (1998). *Comprehensive cellulose chemistry*. Volume 1: Fundamentals and analytical methods. Wiley-VCH Verlag GmbH.

Krässig, H. A. (1993). Cellulose: structure, accessibility, and reactivity. No title.

Krässig, H. (1984). Struktur und reaktivität von cellulosefasern. Papier Darmstadt, 38, 371-582.

Kostag, M., Liebert, T., El Seoud, O. A., & Heinze, T. (2013). Efficient cellulose solvent: quaternary ammonium chlorides. *Macromolecular Rapid Communications, 34(19),* 1580-1584.

Kuga, S. (1980). The porous structure of cellulose gel regenerated from calcium thiocyanate solution. *Journal of Colloid and Interface Science, 77(1),* 413-417.

Lavoine, N., Desloges, I., Dufresne, A., & Bras, J. (2012). Microfibrillated cellulose—Its barrier properties and applications in cellulosic materials: A review. *Carbohydrate Polymers, 90(2),* 735-764.

Lavanya, D., Kulkarni, P., Dixit, M., Raavi, P. K., & Krishna, L. N. V. (2011). Sources of cellulose and their applications—A review. *International Journal of Drug Formulation and Research, 2(1),* 19-38.

Letters, K. (1932). *Viscosimetric analysis on the reaction of cellulose with concentrated zinc chloride solutions.* Kolloid-Zeitschrift, *58(1)*, 229-239.

Lenz, J., Schurz, J., & Wrentschur, E. (1993). Properties and structure of solvent-spun and viscose-type fibres in the swollen state. *Colloid Polymer Science, 271(5),* 460-468.

Li, J., & Wang, Y. (1994). Effect of angelica polysaccharide on bone marrow macrophage and its relationship to hematopoietic regulation. Chinese Traditional and Herbal Drugs.

Liebert, T. (2010). Cellulose solvents—remarkable history, bright future. in Cellulose Solvents: For Analysis, Shaping and Chemical Modification *(pp. 3-54). ACS Publications*.

Lindman, B., Karlström, G., & Stigsson, L. (2010). On the mechanism of dissolution of cellulose. *Journal of Molecular Liquids, 156(1),* 76-81.

Lu, X., Mo, X., Guo, H., & Zhang, Y. (2012). Sulfation modification and anticoagulant activity of the polysaccharides obtained from persimmon (Diospyros kaki L.) fruits. *International Journal of Biological Macromolecules, 51(6),* 1189-1195.

Lv, Y., et al. (2012). Rheological properties of cellulose/ionic liquid/dimethylsulfoxide (DMSO) solutions. *Polymer, 53(12),* 2524-2531.

Mandal, A., & Chakrabarty, D. (2017). Synthesis and characterization of nanocellulose reinforced full-interpenetrating polymer network based on poly(vinyl alcohol) and polyacrylamide (both crosslinked) composite films. *Polymer Composites, 38(8),* 1720-1731.

Marsh, J. T., & Wood, F. C. (1945). An introduction to the chemistry of cellulose. No title.

Matyjaszewski, K., & Möller, M. (2012). Polymer science: a comprehensive reference. No title.

Medronho, B., & Lindman, B. (2014). Competing forces during cellulose dissolution: From solvents to mechanisms. *Current Opinion in Colloid & Interface Science, 19(1),* 32-40.

Medronho, B., Romano, A., Miguel, M. G., Stigsson, L., & Lindman, B. (2012). Rationalizing cellulose (in) solubility: reviewing basic physicochemical aspects and role of hydrophobic interactions. *Cellulose, 19(3),* 581-587.

Miyamoto, H., et al. (2009). Structural reorganization of molecular sheets derived from cellulose II by molecular dynamics simulations. *Carbohydrate Research, 344(14),* 1085-1094.

Morgan, A. B., Gilman, J. W. (2013). *An overview of flame retardancy of polymeric materials*: Application, technology, and future directions. Fire and Materials, *37(4),* 259–279 (17) (PDF) Flame Retardant Material Based on Cellulose Scaffold Mineralized by Calcium Carbonate.

Montgomery Jr, J. A., Frisch, M. J., Ochterski, J. W., & Petersson, G. A. (1999). A complete basis set model chemistry. VI. Use of density functional geometries and frequencies. *Journal of Chemical Physics, 110(6),* 2822-2827.

Montgomery Jr, J. A., Frisch, M. J., Ochterski, J. W., & Petersson, G. A. (2000). A complete basis set model chemistry. VII. Use of the minimum population localization method. *Journal of Chemical Physics, 112(15),* 6532-6542.

Möhl, C., et al. (2022). Development of natural fibre-reinforced semi-finished products with bio-based matrix for eco-friendly composites. *Polymers, 14(4),* 698.

Nair, S. S., Zhu, J., Deng, Y., & Ragauskas, A. J. (2014). High performance green barriers based on nanocellulose. *Sustainable Chemical Processes, 2(1),* 1-7.

Nakagaito, A. N., & Yano, H. (2008). The effect of fiber content on the mechanical and thermal expansion properties of biocomposites based on microfibrillated cellulose. *Cellulose, 15(4),* 555-559.

Nishiyama, Y., Langan, P., & Chanzy, H. (2002). Crystal structure and hydrogen-bonding system in cellulose Iβ from synchrotron X-ray and neutron fiber diffraction. *Journal of the American Chemical Society, 124(31),* 9074-9082.

Northolt, M., et al. (2001). The structure and properties of cellulose fibres spun from an anisotropic phosphoric acid solution. *Polymer, 42(20),* 8249-8264.

Oh, S. Y., et al. (2002). Preparation of regenerated cellulose fiber via carbonation. I. Carbonation and dissolution in an aqueous NaOH solution. *Fibers and Polymers, 3(1),* 1-7.

Oh, S. Y., et al. (2005). Preparation of regenerated cellulose fiber via carbonation (II) Spinning and characterization. *Fibers and Polymers, 6(2),* 95-102.

Olsson, C., & Westman, G. (2013). Direct dissolution of cellulose: background, means, and applications. Cellulose-Fundamental Aspects, 10(52144).

Oosterveld, A., Beldman, G., & Voragen, A. G. (2002). Enzymatic modification of pectic polysaccharides obtained from sugar beet pulp. *Carbohydrate Polymers, 48(1),* 73-81.

Perepelkin, K. (2007). Lyocell fibres based on direct dissolution of cellulose in N-methylmorpholine N-oxide: development and prospects. *Fibre Chemistry, 39(3),* 163-172.

Phanthong, P., et al. (2018). Nanocellulose: Extraction and application. *Carbon Resource Conversion, 1(1),* 32-43.

Pinkert, A., Marsh, K. N., Pang, S., & Staiger, M. P. (2009). Ionic liquids and their interaction with cellulose. *Chemical Reviews, 109(12),* 6712-6728.

Pople, J. A., Gill, P. M., & Johnson, B. G. (1992). Kohn—Sham density-functional theory within a finite basis set. *Chemical Physics Letters, 199(5-6),* 557-560.

Popa, V. (2011). *Polysaccharides in medicinal and pharmaceutical applications*. Smithers Rapra.

Potthast, A., et al. (2002). The cellulose solvent system N, N-dimethylacetamide/lithium chloride revisited: the effect of water on physicochemical properties and chemical stability. *Cellulose, 9(1),* 41-53.

Qiu, S., et al. (2014). Optimization of selenylation conditions for lycium barbarum polysaccharide based on antioxidant activity. *Carbohydrate Polymers, 103,* 148-153.

Ragauskas, A. J., et al. (2006). The path forward for biofuels and biomaterials. *Science, 311(5760),* 484-489.

Röder, T., Moosbauer, J., Wöss, K., Schlader, S., & Kraft, G. (2013). Man-made cellulose fibres—a comparison based on morphology and mechanical properties. *Lenzinger Berichte, 91,* 7-12.

Rosenau, T., Potthast, A., Hofinger, A., Sixta, H., & Kosma, P. (2001). *Hydrolytic processes and condensation reactions in the cellulose solvent system N, N-dimethylacetamide/lithium chloride*. Part 1.

Rosenau, T., Potthast, A., Sixta, H., & Kosma, P. (2001). The chemistry of side reactions and byproduct formation in the system NMMO/cellulose (Lyocell process). *Progress in Polymer Science, 26(9),* 1763-1837.

Ruggiero, J., Urbani, R., & Cesàro, A. (1995). Conformational features of galacturonans. II. Configurational statistics of pectic polymers. *International Journal of Biological Macromolecules, 17(3),* 213-218.

Schulz, L., Seger, B., & Burchard, W. (2000). Structures of cellulose in solution. *Macromolecular Chemistry and Physics, 201(10), 2008-2022.*

Schulze, P., et al. (2016). Incorporation of hydrophobic dyes within cellulose acetate and acetate phthalate based nanoparticles. *Macromolecular Chemistry and Physics, 217(17),* 1823-1833.

Shanbhag, A., Barclay, B., Koziara, J., & Shivanand, P. (2007). Application of cellulose acetate butyrate-based membrane for osmotic drug delivery. *Cellulose, 14(1),* 65-71.

Siddiqui, K. S., & Cavicchioli, R. (2005). Improved thermal stability and activity in the cold-adapted lipase B from Candida antarctica following chemical modification with oxidized polysaccharides. *Extremophiles, 9(6),* 471-476.

Si, J., Cui, Z., Wang, Q., Liu, Q., & Liu, C. (2016). Biomimetic composite scaffolds based on mineralization of hydroxyapatite on electrospun poly(ε-caprolactone)/nanocellulose fibers. *Carbohydrate Polymers, 143,* 270-278.

Siró, I., & Plackett, D. (2010). Microfibrillated cellulose and new nanocomposite materials: *A review. Cellulose, 17(3),* 459-494.

Sixta, H., et al. (2015). Ioncell-F: a high-strength regenerated cellulose fibre. *Nordic Pulp & Paper Research Journal, 30(1),* 43-57.

Sixta, H., Potthast, A., & Krotschek, A. W. (2006). *Chemical pulping processes*. Handbook of Pulp, 1.

Solomon, B. D., Barnes, J. R., & Halvorsen, K. E. (2007). Grain and cellulosic ethanol: History, economics, and energy policy. *Biomass and Bioenergy, 31(6),* 416-425.

Stephens, P. J., Devlin, F. J., Chabalowski, C. F., & Frisch, M. J. (1994). Ab initio calculation of vibrational absorption and circular dichroism spectra using density functional force fields. *Journal of Physical Chemistry, 98(45),* 11623-11627.

Striegel, A. (1997). Theory and applications of DMAc/LiCl in the analysis of polysaccharides. *Carbohydrate Polymers, 34(4),* 267-274.

Swatloski, R. P., Spear, S. K., Holbrey, J. D., & Rogers, R. D. (2002). Dissolution of cellulose with ionic liquids. *Journal of the American Chemical Society, 124(18),* 4974-4975.

Trifol, J., et al. (2016). Hybrid poly(lactic acid)/nanocellulose/nanoclay composites with synergistically enhanced barrier properties and improved thermomechanical resistance. *Polymer International, 65(12),* 988-995.

Ukai, S., Hara, C., Kuruma, I., & Tanaka, Y. (1983). Polysaccharides in fungi. XIV. Anti-inflammatory effect of the polysaccharides from the fruit bodies of several fungi. *Journal of Pharmacobiodynamics, 6(12),* 983-990.

Varshney, V., & Naithani, S. (2011). Chemical functionalization of cellulose derived from nonconventional sources. Cellulose Fibers: Bio- and Nano-Polymer Composites: *Green Chemistry and Technology,* 43-60.

Wang, X., Zhang, Z., Yao, Z., Zhao, M., & Qi, H. (2013). Sulfation, anticoagulant and antioxidant activities of polysaccharide from green algae Enteromorpha linza. *International Journal of Biological Macromolecules, 58,* 225-230.

Wendler, F., Graneß, G., & Heinze, T. (2005). Characterization of autocatalytic reactions in modified cellulose/NMMO solutions by thermal analysis and UV/VIS spectroscopy. *Cellulose, 12(4),* 411-422.

Wendler, F., Kolbe, A., Kraft, J., Einax, J. W., & Heinze, T. (2008). Thermal stability of lyocell solutions: Experimental results and modeling using cluster analysis and partial least squares regression. *Macromolecular Theory and Simulations, 17(1),* 32-38.

Wendler, F., Todi, L.-N., & Meister, F. (2012). Thermostability of imidazolium ionic liquids as direct solvents for cellulose. *Thermochimica Acta, 528,* 76-84.

Woodings, C. (1995). The development of advanced cellulosic fibres. *International Journal of Biological Macromolecules, 17(4-5),* 305-309.

Wu, Q.-X., Zhang, Q.-L., Lin, D.-Q., & Yao, S.-J. (2013). Characterization of novel lactoferrin loaded capsules prepared with polyelectrolyte complexes. *International Journal of Pharmaceutics, 455,* 124-131.

Yamane, C., et al. (2006). Two different surface properties of regenerated cellulose due to structural anisotropy. *Polymer Journal, 38(9),* 819-826.

Yamashiki, T., et al. (1992). New class of cellulose fiber spun from the novel solution of cellulose by wet spinning method. *Journal of Applied Polymer Science, 44(4),* 691-698.

Yang, Y.-J., et al. (2002). Cellulose dissolution in aqueous lithium bromide solutions.

Ye, M., Yuan, R., He, Y., Du, Z., & Ma, X. (2013). Phosphorylation and anti-tumor activity of exopolysaccharide from Lachnum YM120. *Carbohydrate Polymers, 97,* 690-694.

Yu, D., Hu, Y., Zhang, G., Li, W., & Jiang, Y. (2022). *Theoretical studies on the two-photon absorption of II–VI semiconductor nano clusters.* Scientific Reports, *12(1),* 110.

Zhang, L., Ruan, D., & Gao, S. (2002). Dissolution and regeneration of cellulose in NaOH/thiourea aqueous solution. *Journal of Polymer Science Part B: Polymer Physics, 40(16),* 1521-1529.

Zhang, Z., Wang, X., Mo, X., & Qi, H. (2013). Degradation and the antioxidant activity of polysaccharide from Enteromorpha linza. *Carbohydrate Polymers, 92,* 2084-2087.

Zimmermann, M. V. G., da Silva, M. P., Zattera, A. J., & Campomanes Santana, R. M. (2017). Effect of nanocellulose fibers and acetylated nanocellulose fibers on properties of poly(ethylene-co-vinyl acetate) foams. *Journal of Applied Polymer Science, 134(1).*

CURRICULUM VITAE

Uchechukwu Gospel Ariwodo

Email: *uariwodo@pvamu.edu, ariwodogospel94@gmail.com*

Education

- Prairie View A&M University,
  Prairie View, Texas
  Master of Science in Chemistry

- Abia State University, Uturu
  Abia State Nigeria
  Bachelor of Science in Biochemistry

Work Experience

Graduate Research Assistant — Prairie View, TX
Prairie View A&M University

- Characterize the behavior of the cellulose model in sodium salts using a computational approach.
- Predict the peak shift and degradation rate in the mixture of cellulose model and sodium salts using FTIR and TG-DTA.
- Characterize the crystalline structures of Aniline, Pyridine, 2-amino pyridine, and 2,6-diamino pyridine using DSC.
- Synthesize and purify organic compounds using Combi flash and TLC.
- Elucidate the masses of many polar organic compounds using ESI.

Quality Control Analyst — Abia State Nigeria
Anco Heritage Limited

- Treated water samples regularly to evaluate a range of factors, including chemical composition, microbiological contamination, pH, turbidity, and chlorine levels, among other quality indicators.
- Ensured strict regulatory rules placed by the government were followed in water production.
- Collaborated closely with the company's other departments—production, maintenance, and regulatory affairs, for example—to plan quality control initiatives and guarantee overall operational efficacy.

Skills

- Spectroscopic techniques such as FT-IR, NMR, ESI, and GC-MS, Computational application, Avogadro software, GuassView 6.0, Gaussian 09W, Chemdraw, Pymol, and Microsoft Office.

Publications

Nwaogwugwu, C. J., Nwankwo, V. C., Chidi, N. I., Nwaogwugwu, C., **Ariwodo, U. G.,** Chukwuemeka, I., & Nwokoma, F. (2023). Effects Of Alcoholic Leaf Extract of Hunteria Umbellate On Various Parameters In Wistar Female Rats Exposed To Trichloroethylene (TCE). *Journal of Namibian Studies: History Politics Culture*, *34*, 2521-2537.